Eur. Phys. J. A **11**, 441–455 (2001)

THE EUROPEAN PHYSICAL JOURNAL A

Photoproduction of positive pions from hydrogen at large angles in the energy range 0.3–2.0 GeV

H.W. Dannhausen[a], E.J. Durwen[b], H.M. Fischer[c], M. Leneke[d], W. Niehaus[e], and F. Takasaki[f]

Physikalisches Institut, Universität Bonn, D-53115 Bonn, Germany

Received: 2 February 2000 / Revised version: 16 July 2001
Communicated by Th. Walcher

Abstract. The differential cross-section for the reaction $\gamma p \to \pi^+ n$ was measured using the bremsstrahlung beam of the Bonn 2.5 GeV electron synchrotron. The pions were detected and momentum analysed in a multichannel magnet spectrometer. Data reduction resulted in 1278 measured cross-sections which are presented as energy distributions at six laboratory angles between 180° and 95°. The range of laboratory photon energies extended from 0.3 to 2.1 GeV. The statistical accuracy is better than 3 percent, the systematic error is about 5 percent. The data are compared with other experimental results and predictions of a phenomenological analysis. These cross-sections are the result of a measurement program which was started in the seventies. Further results will be reported in forthcoming publications.

PACS. 13.60.Le Meson production – 25.20.Lj Photoproduction reactions

1 Introduction

Pion photoproduction up to 2 GeV incident photon energy is dominated by the formation of nucleon resonances in the s-channel. These objects have been studied extensively in πN-scattering experiments, but the electromagnetic structure of such resonant states can only be analysed through photon excitation. In order to obtain the photocouplings of the individual resonances, the photoproduction amplitudes must be evaluated by a partial-wave analysis of the experimental data. To do this without theoretical assumptions we need in principle seven independent measurements for each process, and for a proper isospin decomposition this must be done for three out of the four $\gamma N \to \pi N$ processes. The quality of such an analysis depends to a high degree on the completeness and consistency of the data used in the fit procedure.

During the last four decades a considerable amount of pion photoproduction data [1] has been accumulated, and a number of analyses [2] have been carried out. Due to the historical development of accelerator technique, the region of the first resonance was investigated first. Later on, the measurements could be extended to the region of the second, third and fourth resonance up to about 1.4 GeV so that also in this energy range we have now abundant information. Beyond this energy the coverage in angle and energy for most of the observables is still insufficient. This applies also to the differential cross-section of positive pion photoproduction where only some measurements at small and large angles exist [1].

Measurements in the backward hemisphere are of special interest because the non-resonant background is much smaller than at forward angles, where the one-pion-exchange term gives large contributions. The excitation curve at 180° is of particular importance. At this angle the transition amplitude takes an exceptional simple form, out of four helicity amplitudes only contributions of the one having helicity 1/2 do appear. For these reasons an experiment was set up at the Bonn 2.5 GeV electron synchrotron to measure the differential cross-section for the reaction $\gamma p \to \pi^+ n$ preferably at backward angles including the laboratory angle of 180°. The aim was to take a consistent data set with high statistics, a minimum of systematic errors, and good energy resolution. The measurements presented here were made at six pion laboratory angles between 180° and 90° and photon laboratory energies covering the wide energy range from 0.3 to 2.1 GeV.

2 Experimental method

Positive pions were photoproduced by a bremsstrahlung beam incident on a liquid hydrogen target. The produc-

[a] *Present address*: Diakonie-Krankenhaus, 27356 Rotenburg/Wümme, Germany.
[b] *Present address*: Mannesmann Mobilfunk GmbH, 40547 Düsseldorf, Germany.
[c] e-mail: `fischer@physik.uni-bonn.de`
[d] Deceased.
[e] *Present address*: Bundesamt für Wehrtechnik und Beschaffung, 56073 Koblenz, Germany.
[f] *Present address*: National Laboratory for High Energy Physics, KEK, Tsukuba, 305, Japan.

tion angle Θ and the momentum p of the particles were analysed in a magnetic spectrometer. Data were taken in energy scans at six fixed laboratory angles [3]. This implied that the corresponding CM angles varied with photon energy, as shown in fig. 1. This procedure was chosen for two reasons. In the first place, a change of the angular position of the spectrometer required the break of the vacuum system between the target vessel and the detector. A continuous adjustment of the laboratory angle therefore would have led to unbearable delays in data taking. Secondly, the spectrometer collected data in 24 adjacent momentum channels simultaneously, a feature which also favoured the measurement of excitation curves at fixed laboratory angle.

Each energy scan between 0.3 GeV and 2.0 GeV required several settings of the central momentum. For each, an appropriate value for the synchrotron energy E_0 was chosen. Consecutive settings were selected so that the momentum acceptance covered half the range of the previous measurement. Thus, for each photon energy two independent measurements were carried out, however, with different parts of the momentum acceptance. This double coverage proved to be very useful for checking the consistency of the acceptance calculations and the adjustment of the system. For each combination of pion angle and momentum a minimum photon energy is needed to produce an additional pion in the reaction $\gamma p \to \pi^+\pi^- p$ or $\gamma p \to \pi^+\pi^0 n$. For all our measurements, the synchrotron energy E_0 was always kept below this threshold so that multiple pion reactions could not be registered.

The background incident on the spectrometer consisted of protons, positive muons and positrons. The protons were separated from pions by time-of-flight measurements between scintillation counters. Muons originating from pion decay could not be distinguished from pions. The loss of pions due to decay and the resulting muon contamination were calculated with a Monte Carlo technique. The positron yield from pair production in hydrogen was calculated to be negligible. As an additional check, measurements with reversed polarity of the magnet were carried out.

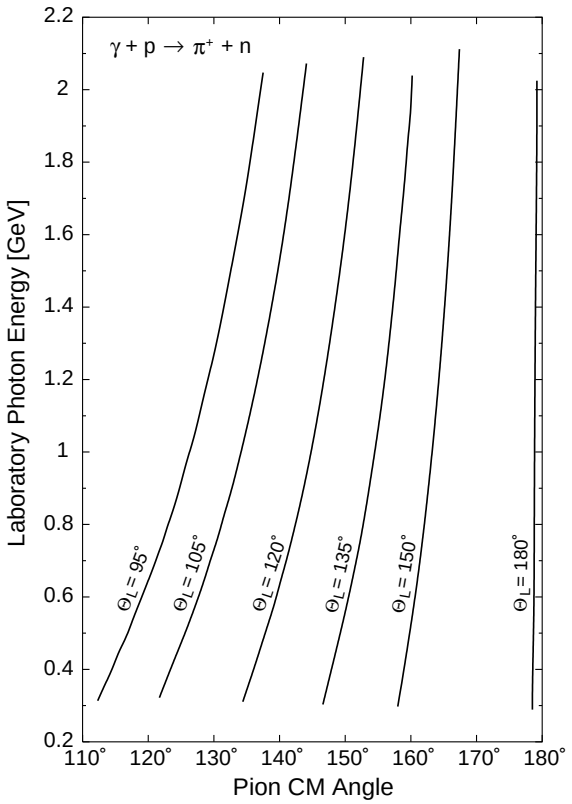

Fig. 1. Kinematics of pion photoproduction from hydrogen. The photon energies are plotted as a function of the CM angle for all laboratory angles where excitation curves were measured.

3 Experimental arrangement

The experiment was carried out using a bremsstrahlung beam of the Bonn 2.5 GeV synchrotron [4]. Positive pions produced in a liquid-hydrogen target were identified and momentum analysed with the 0.62 GeV/c spectrometer ATHOS. The layout of the experimental area is shown in fig. 2. The detailed aspects of the experiment are discussed below.

3.1 Photon beam and hydrogen target

The internal electron beam of the synchrotron irradiated a tungsten radiator of 1 mm diameter 10 m upstream from the hydrogen target used in this experiment. The resulting bremsstrahlung beam was collimated by the lead collimator C_1 to a rectangular cross-section with half angles of 0.9 and 0.5 mrad. The two lead scrapers C_2 and C_3 and the first sweeping magnet cleaned the beam of charged particles before entering the spectrometer area. C_2 and C_3 had slightly larger apertures than the profile of the photon beam defined by C_1. After passing through the hydrogen target, the beam flux was measured in a Wilson-type quantameter [5]. A second cleaning magnet behind the hydrogen target removed particles scattered back from the quantameter. This was of vital importance for the measurements at 180°. The shape of the photon spectrum for each electron energy E_0 was calculated by a computer program using formulae compiled by Lublow [6]. Collimation effects were taken into account according to Lutz and Schultz [7]. The obtained spectra were estimated to be accurate to better than one percent. In order to avoid errors due to uncertainties in the shape of the spectra near the upper end, the used energy was always kept below 0.9 E_0. The intensity profile of the photon beam was surveyed by means of silver-phosphate glasses [8] at several synchrotron energies. The alignment of the photon beam was checked by Polaroid pictures any time when the accelerator parameters were changed.

The liquid-hydrogen target was contained in a cylindrical Mylar cup 6 cm in diameter and 10 cm high. The axis

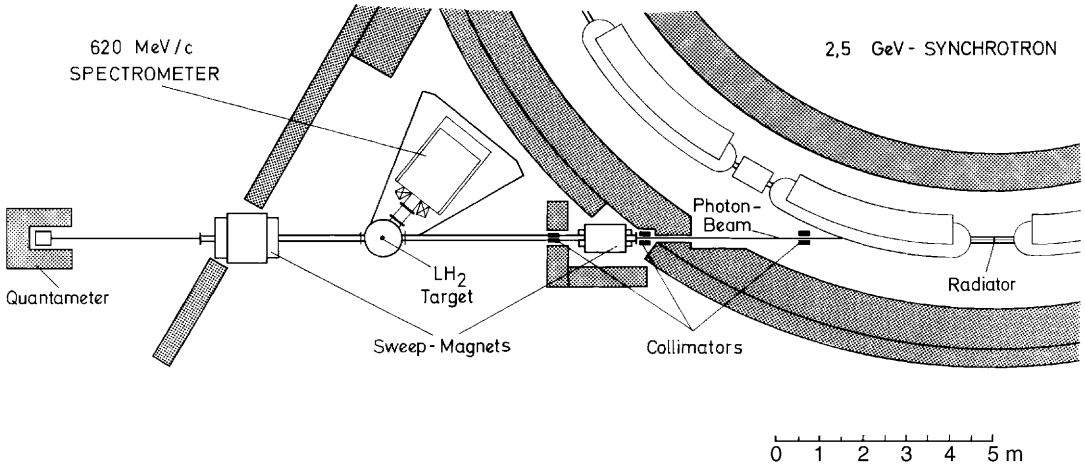

Fig. 2. Layout of the experimental area.

of the cup was vertical and perpendicular to the production plane defined by the photon beam and the spectrometer central trajectory. To prevent the residual gas from condensation on the cold walls of the target cup, an additional cell made of 7.5 μm Hostaphan foil was installed. It surrounded the hydrogen cell at a distance of 2 cm. The gap between the two foils was connected to the main vacuum system by a thin pipe only. By this provision, the formation of ice on the hydrogen cell could be kept at a negligible rate during a three weeks run. The target vessel was integrated into an extended vacuum system with a total volume of 1 m^3. It covered the photon beam line between the two cleaning magnets and also the pion trajectories inside the spectrometer up to the front of the scintillation counter S2. The target vessel was equipped with a series of flanges to allow measurements at different angles. The vacuum chamber of the spectrometer could be connected to the target vessel at intervals of five degrees and angles between 35° and 155°. With this arrangement the background in the experimental area as well as Coulomb scattering and nuclear absorption of the pions in the spectrometer were reduced to a minimum.

3.2 The magnet spectrometer ATHOS

A side view of the 0.62 GeV/c spectrometer ATHOS used in this experiment is shown in fig. 3. Charged particles emerging from the hydrogen target were deflected in the vertical direction by a wedge-shaped weak focussing magnet. The bend angle was 108°, the gap height at the center 14.5 cm. The pole pieces were 52 cm wide with a mean radius of 110 cm. For an efficient use of the field volume the pole pieces were incorporated into the vacuum chamber. The stainless-steel side walls of the chamber were skilfully soldered to the edges of the poles. The magnet was acquired from LAL Orsay where also the design and calibration had been carried out [9].

There were two connecting pipes through the iron yoke to the vacuum chamber. One of the two was oriented tangentially to the central orbit at the entrance face of the

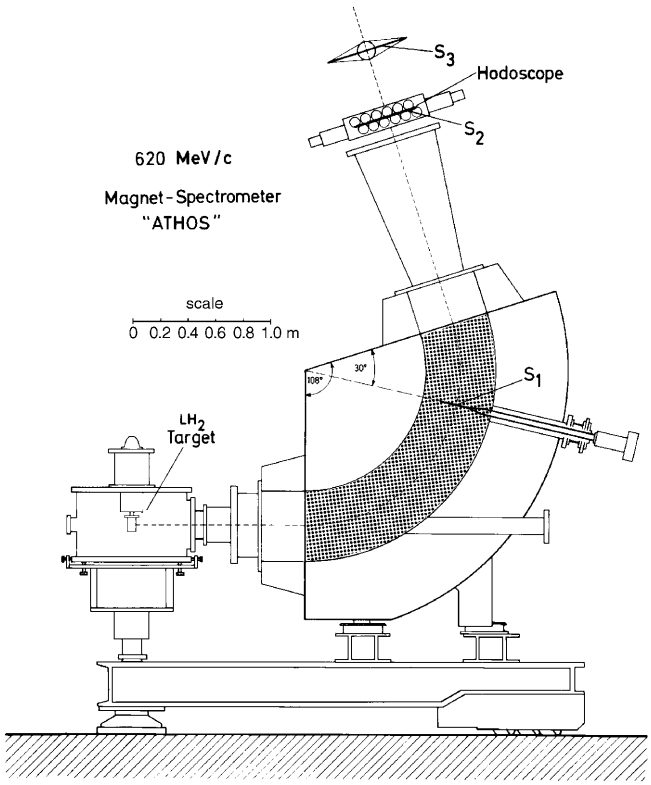

Fig. 3. Side view of the magnet spectrometer ATHOS.

magnet. Using this as entrance port for the photon beam enabled us to do the measurements at a production angle of 180°. The second one pointing radially at 30° relative to the exit face permitted an easy installation of an aperture counter inside the vacuum chamber.

At maximum induction of 1.835 T the central momentum was 0.608 GeV/c. The poles were shaped to give a first- and second-order field index of $n = 0.316$ and $\beta = 0.10$ which showed a small but predictable change with magnet excitation. The inclination and curvature of the effective field boundaries were corrected by shims on

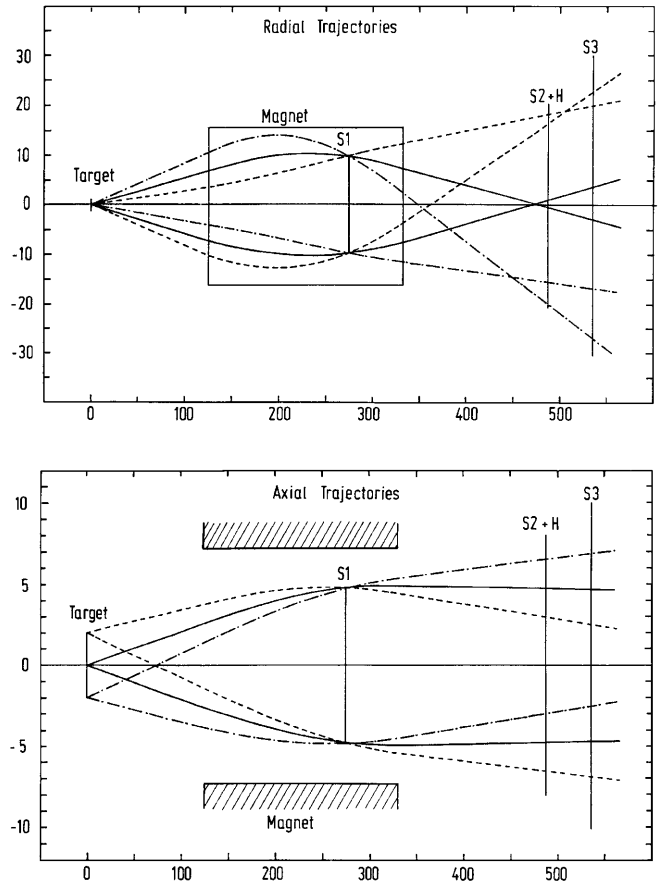

Fig. 4. Calculated trajectories through the spectrometer for initial values of horizontal and vertical angles, horizontal positions and momentum deviations.

the pole faces so that they coincided with the geometrical dimensions of the iron. The optical properties of the spectrometer are illustrated in fig. 4. In first-order optics the sector magnet was parallel-to-point focusing in the horizontal plane. In the momentum dispersing (vertical) plane there was point-to-point focusing. The hydrogen target was placed at a distance of 125 cm from the magnet entrance face. Counter S2 was located at the proper first-order focus at 144 cm behind the magnet. The position of the end counter S3 was at 192 cm. Its size was larger than necessary so that the acceptance was only determined by the dimensions of S2. The dimensions of the aperture defining counter S1 were chosen to retain all possible particle trajectories within the useful field volume and also to exclude particles scattered from the pole faces from detection. These requirements were met by a scintillator of $10 \times 20\,\mathrm{cm}^2$ which resulted in an angle acceptance of 46 mrad in the horizontal plane, 113 mrad in the vertical plane, and an average solid angle of the spectrometer of $\Delta\Omega = 5.2$ msterad.

Particles leaving the target with a given momentum were focused along a line in the momentum focal plane with a dispersion of 3.4 cm per percent momentum variation relative to the central trajectory. The position in this plane and thus the momentum of the particles were measured by a momentum hodoscope. In first order the focal plane was perpendicular to the central trajectory. Second-order terms caused an inclination of 30.5° relative to the central trajectory. For technical reasons the 24 channel momentum hodoscope in front of S2 was mounted perpendicular to the central trajectory. As a consequence, the momentum resolution of the individual channels was not constant but varied between 0.5% and 1.4% FWHM. For each setting of momentum and synchrotron energy, the acceptance of all channels were determined by Monte Carlo calculations.

3.3 Electronics and on-line data processing

Pions were identified by a coincidence of the photomultiplier signals of counters S1, S2 and S3. The light produced in the scintillator of S2 was collected from two sides, and the respective PM signals S2.1 and S2.2 were mixed before they were fed into the triple coincidence S1 × S2.mix × S3 to define a pion trigger. An additional parallel logic-coincidence circuit with a 100 ns delay for signal S1 was used as a measure for the accidental-coincidence rate. A logic "OR" of the pion and the accidental-coincidence signals provided the general trigger which initialised the reading of the 24-bit hit pattern of the hodoscope as well as the time-of-flight measurement between counter S1 and S3 and also the pulse height measurement of S1, S2.1, S2.2, S2.mix and S3. For each general trigger, this information and, in addition, the contents of scalers for the quantameter rate and the time elapsed between consecutive events were transferred to an on-line computer via a CAMAC interface, and finally written on magnetic tapes for further off-line analysis. For a real-time check of the experimental parameters, the computer performed an on-line data reduction in order to display various listings, histograms and spectra. In addition, all voltages needed for the experiment were automatically checked by the computer.

4 Data collection and reduction

4.1 Experimental procedure

For each laboratory angle about 16 different settings of the spectrometer momentum and synchrotron energy were needed to cover the whole energy range. At photon energies above 0.7 GeV, we determined the cross-section for each individual hodoscope channel. Below that energy one single cross-section was calculated from the rates of two to six adjacent hodoscope channels in order to obtain a nearly constant photon-energy resolution. At energies above 1.5 GeV the energy range accepted by the spectrometer extended below the two-pion production threshold. In this case, only the data from the high-energy part of the hodoscope above this threshold was evaluated. The empty target background was measured for each setting and subtracted from the full target rates. It showed only a weak energy dependence. Up to 1 GeV photon energy

it amounted to typically 2 to 4 percent of the full target rate, and increased to 8 to 12 percent in the high-energy region. The increase of this ratio was mainly caused by the strong decrease of the differential cross-section towards higher energies. An extreme value of 46 percent was found for $\Theta = 180°$ at 1.7 GeV photon energy where the pion production shows a dip.

4.2 Corrections

The net pion rates were corrected for counting losses due to nuclear absorption in the target and the counter system, for pion decay as well as for muon contamination, and counts caused by back-scattering of forward-produced pions in the hydrogen target.

The nuclear absorption correction was evaluated following the scheme of Thiessen [10]. The fraction of pions lost by nuclear interactions is shown in fig. 5. The relative uncertainty of this calculation was estimated to be about 25% which in turn caused a maximum error of the cross-section of 1.2%. At maximum momentum, 15 percent of the emitted pions decayed during their flight through the spectrometer. At the minimum detected momentum, only the fraction of $R_\pi = 0.5$ could reach counter S3. The ratio R_π as a function of the pion momentum is shown in fig. 6 together with R_μ and $R_{\pi\mu}$. The decay muons were emitted into a narrow forward cone so that some of them could continue through the counter system of the spectrometer and trigger the electronics. These events could not be distinguished from pions. The fraction R_μ of emitted pions which led to such a muon contamination was calculated in a Monte Carlo program. The total correction due to pion decay is given by $R_{\pi\mu} = R_\pi + R_\mu$. The momentum dependence of these three quantities is shown in fig. 6.

It was pointed out by d'Almagne [11] that pions originally produced in forward directions can be scattered from target nucleons into the acceptance of the spectrometer at large angles and thus give rise to a non-negligible contamination. There was again no means to separate these particles from the ones which were emitted directly into the spectrometer acceptance. The probabilities for the detection of these "phantom" pions were determined by simulating this process on the computer. Figure 7 shows the fraction of phantom pions contained in the counting rate for various laboratory angles. The uncertainty of this correction was estimated to be 20% . This contamination was especially large for the 180° measurements. The bump at 0.450 GeV is due to the large pion nucleon cross-section at this energy, whereas the peak at 1.7 GeV is again due to the dip in the photoproduction cross-section.

Effects of multiple hits in the hodoscope, gating during processing time of the on-line computer, accidentals and the influence of the finite resolutions on the cross-section were carefully investigated. The corresponding corrections turned out to be:

multiple hits	1–3% ,
gating	0–2.8% ,
accidentals	$< 1\%$,
resolution	0–3% .

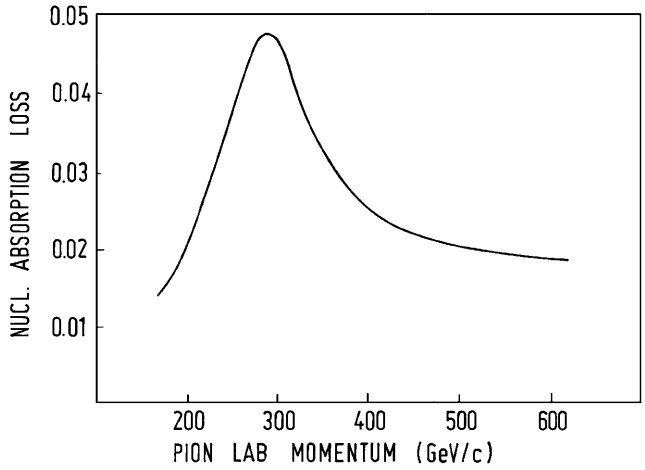

Fig. 5. Nuclear absorption correction as a function of the pion laboratory momentum.

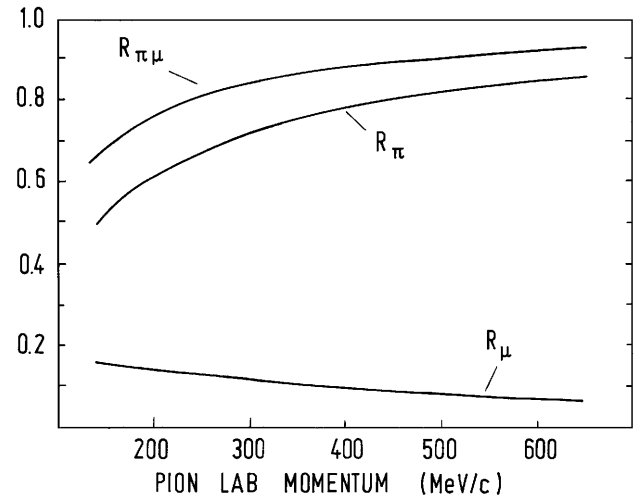

Fig. 6. Ratio of pion decay R_π, muon contamination R_μ and total rate reduction $R_{\mu\pi} = R_\pi + R_\mu$ as a function of the pion momentum.

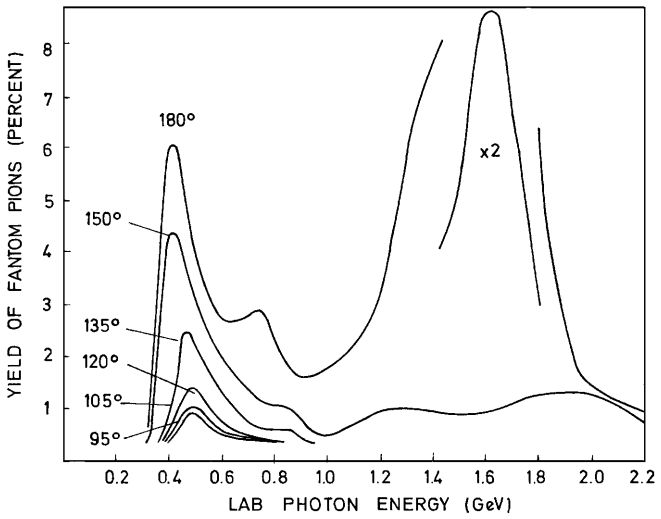

Fig. 7. Yield of back-scattered pions as a function of the laboratory photon energy.

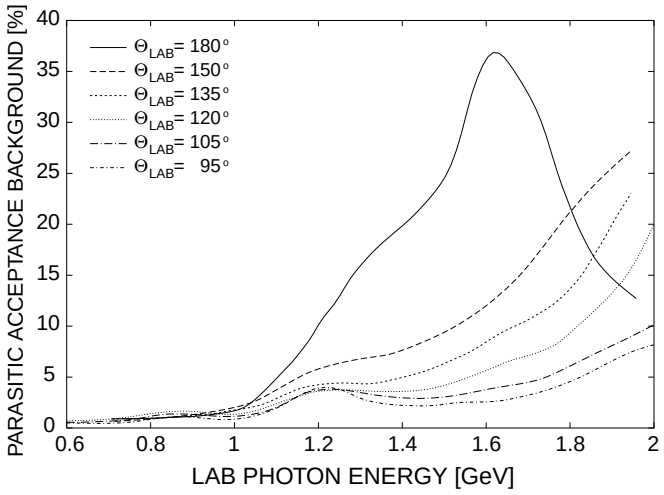

Fig. 8. Fractions of the parasitic acceptance background as a function of the laboratory photon energy.

An extensive program was carried out parallel to data taking runs to check the acceptance calculations and the momentum calibration. Various yield curves for fixed synchrotron energies E_0 were measured as a function of the spectrometer momentum. The acceptances and the calibration proved to be correct but through this procedure a new type of background was observed. When the spectrometer momentum was raised to such values that the corresponding photon energies exceeded the maximum energy E_0, a non-vanishing yield of positive particles remained after subtraction of the empty target rates. After a large number of tests, the origin and the identity of these particles could finally be established. This intriguing background consisted out of positive pions which were produced in the hydrogen target and emitted towards the coils above the pole tips outside the regular acceptance. The pions could pass through a hidden slit between the coils, penetrate the wall of the vacuum chamber, hit the aperture counter S1, and finally reach the other counters after proper deflection by the magnetic field. These particles showed a broad momentum distribution with a center value 14% below the central spectrometer momentum. This could be determined through range measurements behind counter S4. After installation of a proper lead shielding around the coils this background disappeared.

In order to develop a suitable correction procedure for the data already collected the particle flux through this extra acceptance was investigated under various conditions by computer simulations. A fairly satisfactory description of the effect could eventually be reached by extending the momentum acceptance of each hodoscope channel towards smaller momenta by adding a linearly decaying tail to the roughly Gaussian regular acceptance function. The range and slope of this extension could be determined from the measured yield curves. Fractions of this parasitic acceptance background as a function of photon energy are shown in fig. 8. For photon energies up to 1.0 GeV, the calculated corrections were less than two percent of the measured pion rates at all angles. At higher energies we observed a strong dependence on the pion angle. For the excitation curves at 95° and 105° the correction amounted to 5% at 1.8 GeV and 8%–10% at 2.0 GeV. For the measurements at laboratory angles of 120°, 135° and 150° we obtained corrections of 4%–8% at $E_\gamma = 1.5$ GeV with a steep increase to 20%–28% at 2 GeV. At $\Theta = 180°$ this correction was exceptionally large. It rose almost linearly to 35% at 1.6 GeV, where the cross-sections itself shows its minimum, and then dropped down again to 10% at $E_\gamma = 2$ GeV. Because of the somewhat simplified assumptions and some uncertainties in the determination of the parameters, the relative uncertainty of these corrections was estimated to be 20 percent.

5 Results and discussion

5.1 Results of this experiment

The cross-sections measured in this experiment are plotted in figs. 9 to 14, and listed in table 1 as excitation curves at fixed laboratory angles. The errors quoted with the cross-sections include counting statistics and the uncertainties of the parasitic acceptance correction but no other systematic errors. The photon-energy resolution $\Delta k/k$ depends on the pion laboratory angle and the photon energy. It varied from 1.5% (FWHM) at $\Theta = 180°$ in the first resonance region up to 8.5% (FWHM) at 2.0 GeV for $\Theta = 95°$. The angular resolution was typically 1.7° (FWHM) and reached a maximum of 2.3° (FWHM) at $\Theta = 180°$. All excitation curves show a general decrease with energy superimposed by maxima around 0.3 GeV, 0.7 GeV, 1.0 GeV and 1.4 GeV known as the first, second, third, and fourth resonance. In order to display adequately the structures in the cross-sections at all energies, the data around the first resonance were reduced to 1/4. Above the third resonance the cross-sections are in addition plotted after multiplication by 4.

Measurements at backward angles are especially useful for the study of the resonances in the low partial waves which are, in general, veiled by the dominant resonance contributions in the higher waves. By angular momentum conservation at an angle of 180°, all helicity amplitudes vanish but H_4 which corresponds to an initial helicity 1/2. As was first observed by Walker [12], the second and third resonances occur almost entirely in the amplitudes corresponding to initial helicity 3/2, and thus show little effect on the backward cross-section. In addition, the t-channel term of the electric Born approximation which contains high partial waves also vanishes at 180°. The remaining electric and magnetic Born terms only affect the lowest partial waves.

Looking at the excitation curve at $\Theta = 180°$ (fig. 9) we notice the following features. Above 0.3 GeV the data show the steep slope of the high-energy tail of the first resonance up to about 0.5 GeV. In the following range, up to 1 GeV, the cross-section in general decreases slowly and then drops rapidly towards higher energies. After a shallow minimum around 1.65 GeV the cross-section

Table 1. The measured values of the CM differential cross-sections $\mathrm{d}\sigma/\mathrm{d}\Omega$ in μb/sr and the associated statistical errors for the reaction $\gamma p \to \pi^+ n$. k_{Lab} is the laboratory photon energy, $\Theta_{\mathrm{C\,M}}$ the pion CM angle and $W_{\mathrm{C\,M}}$ the total energy. The different settings are indicated in the last column.

Pion-Lab.-Angle: 180 Degree

k_{lab} [GeV]	W_{CM} [GeV]	Θ_{CM} [deg.]	$d\sigma/d\Omega$ [μb/st]	Error [μb/st]	#
0.289	1.193	178.5	17.465	0.422	1
0.296	1.198	178.5	17.965	0.418	1
0.304	1.205	178.5	17.840	0.407	1
0.308	1.208	178.5	15.767	0.260	2
0.313	1.211	178.5	16.655	0.380	1
0.316	1.214	178.5	15.799	0.252	2
0.325	1.221	178.5	14.485	0.235	2
0.328	1.223	178.5	14.211	0.330	3
0.336	1.229	178.5	12.926	0.216	2
0.337	1.230	178.5	12.358	0.300	3
0.348	1.238	178.5	10.067	0.275	3
0.349	1.239	178.5	10.881	0.217	4
0.360	1.247	178.5	8.441	0.238	3
0.361	1.248	178.5	8.610	0.197	4
0.371	1.256	178.5	7.746	0.200	5
0.373	1.257	178.5	7.284	0.174	4
0.379	1.262	178.5	6.511	0.187	5
0.387	1.268	178.5	5.816	0.153	4
0.388	1.268	178.5	6.076	0.174	5
0.396	1.274	178.5	5.171	0.126	6
0.398	1.276	178.5	5.220	0.159	5
0.406	1.282	178.5	4.473	0.121	6
0.408	1.283	178.5	4.912	0.150	5
0.416	1.289	178.5	4.301	0.113	6
0.420	1.292	178.5	4.406	0.140	5
0.424	1.295	178.5	3.998	0.121	7
0.427	1.297	178.5	4.120	0.107	6
0.434	1.302	178.5	3.931	0.121	7
0.439	1.305	178.5	3.578	0.103	6
0.446	1.310	178.5	3.560	0.115	7
0.452	1.315	178.5	3.709	0.101	6
0.453	1.315	178.5	3.552	0.101	8
0.458	1.319	178.5	3.569	0.112	7
0.465	1.324	178.5	3.236	0.101	8
0.472	1.329	178.5	3.432	0.105	7
0.479	1.334	178.5	3.213	0.096	8
0.488	1.340	178.5	3.336	0.103	7
0.493	1.344	178.5	3.303	0.094	8
0.509	1.355	178.5	3.217	0.089	8
0.515	1.359	178.6	3.333	0.116	9
0.522	1.364	178.7	3.434	0.115	9
0.527	1.367	178.5	3.220	0.087	8
0.530	1.369	178.7	3.353	0.117	9
0.538	1.375	178.8	3.422	0.114	9
0.547	1.381	178.8	3.448	0.115	9
0.550	1.383	178.6	3.472	0.123	10
0.554	1.386	178.7	3.349	0.121	10
0.556	1.387	178.9	3.267	0.112	9
0.558	1.388	178.7	3.404	0.114	10
0.563	1.392	178.7	3.370	0.116	10

Pion-Lab.-Angle: 180 Degree

k_{lab} [GeV]	W_{CM} [GeV]	Θ_{CM} [deg.]	$d\sigma/d\Omega$ [μb/st]	Error [μb/st]	#
0.565	1.393	178.8	3.450	0.109	9
0.568	1.395	178.7	3.166	0.118	10
0.572	1.398	178.8	3.110	0.115	10
0.575	1.400	178.8	3.216	0.109	9
0.577	1.401	178.8	2.968	0.115	10
0.581	1.404	178.8	3.250	0.113	10
0.585	1.406	178.8	3.178	0.108	9
0.586	1.407	178.8	3.127	0.111	10
0.591	1.410	178.8	3.088	0.113	10
0.596	1.414	178.7	3.081	0.105	9
0.596	1.414	178.9	3.073	0.111	10
0.601	1.417	178.9	3.028	0.108	10
0.607	1.421	178.8	2.978	0.110	10
0.608	1.422	178.7	3.081	0.105	9
0.612	1.424	178.9	3.167	0.109	10
0.615	1.425	178.6	3.108	0.103	11
0.617	1.428	178.7	3.217	0.098	11
0.618	1.428	178.8	2.862	0.112	10
0.620	1.430	178.6	3.151	0.097	9
0.623	1.432	178.7	3.194	0.098	11
0.624	1.432	178.8	2.820	0.104	10
0.628	1.435	178.7	2.871	0.106	11
0.630	1.436	178.8	2.876	0.107	10
0.634	1.439	178.8	3.003	0.099	11
0.635	1.439	178.6	3.110	0.092	12
0.636	1.440	178.8	2.943	0.101	10
0.639	1.442	178.8	2.944	0.099	11
0.641	1.443	178.7	2.887	0.088	12
0.642	1.444	178.7	2.862	0.099	10
0.645	1.446	178.8	2.987	0.095	11
0.647	1.447	178.7	3.023	0.088	12
0.649	1.449	178.8	2.773	0.103	10
0.651	1.450	178.9	2.944	0.090	11
0.652	1.450	178.8	2.927	0.090	12
0.655	1.452	178.7	2.922	0.099	10
0.657	1.454	178.8	2.954	0.094	11
0.658	1.454	178.8	2.958	0.092	12
0.662	1.457	178.6	2.893	0.105	10
0.663	1.458	178.9	2.919	0.089	11
0.664	1.458	178.8	2.895	0.089	12
0.669	1.461	178.9	2.743	0.096	11
0.669	1.461	178.6	2.855	0.102	10
0.670	1.462	178.8	3.081	0.088	12
0.675	1.465	178.9	2.848	0.098	11
0.676	1.466	178.9	2.865	0.089	12
0.677	1.467	178.6	2.849	0.095	10
0.682	1.470	178.9	2.983	0.092	11
0.682	1.470	178.9	2.868	0.088	12
0.689	1.474	178.9	2.978	0.092	11
0.689	1.474	178.9	3.183	0.089	12

Pion-Lab.-Angle: 180 Degree

k_{lab} [GeV]	W_{CM} [GeV]	Θ_{CM} [deg.]	$d\sigma/d\Omega$ [μb/st]	Error [μb/st]	#
0.696	1.479	178.9	3.034	0.086	12
0.696	1.479	178.9	2.981	0.096	11
0.703	1.483	178.9	3.303	0.090	12
0.703	1.483	178.9	3.083	0.100	11
0.710	1.488	178.9	3.188	0.098	12
0.710	1.488	178.9	3.332	0.101	11
0.717	1.492	178.9	3.176	0.087	12
0.718	1.493	178.8	3.047	0.094	11
0.725	1.497	178.9	2.854	0.084	12
0.726	1.498	178.8	2.814	0.088	11
0.732	1.501	178.9	2.650	0.082	12
0.733	1.502	178.8	2.804	0.086	11
0.740	1.506	178.9	2.459	0.079	12
0.742	1.508	178.8	2.629	0.086	11
0.748	1.511	178.8	2.564	0.080	12
0.751	1.513	178.7	2.495	0.083	11
0.757	1.517	178.8	2.417	0.077	12
0.760	1.519	178.7	2.250	0.093	11
0.766	1.522	178.8	2.155	0.075	12
0.767	1.523	178.7	2.446	0.087	13
0.769	1.524	178.6	2.323	0.081	11
0.774	1.527	178.8	2.348	0.076	12
0.775	1.528	178.8	2.286	0.083	13
0.783	1.533	178.8	2.460	0.083	13
0.784	1.533	178.7	2.410	0.074	12
0.791	1.538	178.8	2.283	0.084	13
0.793	1.539	178.7	2.362	0.070	12
0.799	1.543	178.9	2.358	0.087	13
0.803	1.545	178.7	2.414	0.073	12
0.808	1.548	178.9	2.280	0.081	13
0.816	1.553	178.9	2.234	0.083	13
0.825	1.558	178.9	2.318	0.081	13
0.834	1.564	178.9	2.298	0.084	13
0.844	1.570	179.0	2.419	0.084	13
0.853	1.575	179.0	2.483	0.083	13
0.863	1.581	179.0	2.494	0.084	13
0.873	1.587	178.9	2.571	0.083	13
0.884	1.594	179.0	2.718	0.087	13
0.895	1.600	178.9	2.592	0.087	13
0.906	1.606	179.0	2.741	0.085	13
0.918	1.613	178.9	2.602	0.084	13
0.929	1.620	178.9	2.620	0.083	13
0.942	1.627	178.9	2.545	0.081	13
0.950	1.632	179.0	2.576	0.047	14
0.955	1.635	178.9	2.692	0.083	13
0.962	1.639	179.0	2.493	0.045	14
0.969	1.643	178.8	2.449	0.080	13
0.974	1.646	179.0	2.526	0.046	14
0.982	1.650	178.8	2.469	0.080	13
0.987	1.653	179.0	2.407	0.044	14

Pion-Lab.-Angle: 180 Degree

k_{lab} [GeV]	W_{CM} [GeV]	Θ_{CM} [deg.]	$d\sigma/d\Omega$ [μb/st]	Error [μb/st]	#
0.997	1.659	178.8	2.249	0.077	13
0.998	1.659	179.0	2.247	0.043	14
1.012	1.667	178.8	2.074	0.075	13
1.012	1.667	179.0	2.194	0.043	14
1.026	1.675	179.0	2.001	0.041	14
1.039	1.682	179.0	1.762	0.039	14
1.054	1.691	179.0	1.546	0.038	14
1.070	1.699	179.0	1.251	0.035	14
1.085	1.708	179.0	1.021	0.033	14
1.101	1.717	179.0	0.876	0.031	14
1.118	1.726	178.9	0.697	0.029	14
1.136	1.736	178.9	0.605	0.027	14
1.148	1.742	179.1	0.584	0.026	15
1.154	1.745	178.9	0.539	0.026	14
1.165	1.751	179.1	0.545	0.025	15
1.173	1.755	178.9	0.476	0.024	14
1.182	1.760	179.1	0.460	0.024	15
1.193	1.766	178.9	0.376	0.022	14
1.201	1.770	179.1	0.365	0.023	15
1.213	1.777	178.8	0.298	0.020	14
1.220	1.780	179.0	0.323	0.022	15
1.240	1.791	179.1	0.288	0.021	15
1.259	1.801	179.0	0.245	0.019	15
1.281	1.812	179.0	0.195	0.019	15
1.303	1.824	179.0	0.190	0.017	15
1.326	1.835	179.0	0.156	0.016	15
1.351	1.848	179.0	0.144	0.015	15
1.357	1.851	179.1	0.152	0.017	16
1.376	1.861	178.9	0.140	0.014	15
1.380	1.863	179.1	0.149	0.016	16
1.403	1.874	178.9	0.134	0.013	15
1.405	1.875	179.1	0.123	0.015	16
1.430	1.888	178.9	0.088	0.012	15
1.430	1.888	179.1	0.107	0.014	16
1.457	1.901	179.1	0.102	0.013	16
1.486	1.916	179.1	0.079	0.012	16
1.515	1.930	179.1	0.064	0.011	16
1.547	1.945	179.0	0.049	0.010	16
1.580	1.961	179.0	0.033	0.010	16
1.613	1.977	179.0	0.022	0.009	16
1.659	1.998	179.2	0.025	0.010	17
1.691	2.013	179.2	0.029	0.009	17
1.726	2.030	179.2	0.031	0.009	17
1.761	2.046	179.2	0.034	0.008	17
1.800	2.064	179.2	0.042	0.008	17
1.840	2.082	179.2	0.054	0.008	17
1.882	2.100	179.2	0.065	0.007	17
1.927	2.120	179.2	0.068	0.007	17
1.975	2.142	179.2	0.073	0.007	17
2.025	2.163	179.1	0.090	0.007	17

Pion-Lab.-Angle: 150 Degree

k_{lab} [GeV]	W_{CM} [GeV]	Θ_{CM} [deg.]	$d\sigma/d\Omega$ [μb/st]	Error [μb/st]	#
0.297	1.199	158.0	18.031	0.502	1
0.305	1.205	158.1	17.041	0.473	1
0.314	1.212	158.2	16.660	0.459	1
0.323	1.219	158.3	15.276	0.429	1
0.335	1.228	158.4	13.361	0.392	2
0.343	1.235	158.4	12.104	0.365	2
0.352	1.241	158.5	10.762	0.335	2
0.362	1.249	158.6	8.535	0.297	2
0.378	1.261	158.8	6.974	0.244	3
0.387	1.268	158.9	6.090	0.211	3
0.396	1.274	158.9	5.435	0.232	3
0.406	1.282	159.0	5.064	0.185	3
0.416	1.289	159.1	4.489	0.160	3
0.428	1.298	159.2	3.939	0.195	3
0.429	1.298	159.3	4.308	0.132	4
0.440	1.306	159.4	3.724	0.137	4
0.448	1.312	159.4	3.616	0.119	5
0.452	1.315	159.5	3.608	0.127	4
0.456	1.318	159.5	3.454	0.117	5
0.464	1.323	159.6	3.649	0.122	4
0.465	1.324	159.6	3.352	0.114	5
0.475	1.331	159.7	3.335	0.114	5
0.478	1.333	159.7	3.294	0.116	4
0.485	1.338	159.8	3.362	0.113	5
0.494	1.344	159.8	3.428	0.113	4
0.497	1.346	159.9	3.435	0.110	5
0.503	1.351	159.9	3.623	0.106	6
0.509	1.355	160.0	3.341	0.110	5
0.514	1.358	160.0	3.453	0.103	6
0.522	1.364	160.1	3.396	0.107	5
0.525	1.366	160.1	3.346	0.105	6
0.525	1.366	160.1	3.454	0.111	7
0.532	1.371	160.2	3.671	0.119	7
0.537	1.374	160.2	3.474	0.102	6
0.540	1.376	160.3	3.381	0.108	7
0.549	1.382	160.3	3.268	0.121	7
0.550	1.383	160.3	3.395	0.099	6
0.557	1.388	160.4	3.233	0.123	7
0.564	1.392	160.5	3.334	0.098	6
0.566	1.394	160.5	3.232	0.110	7
0.572	1.398	160.4	3.345	0.078	8
0.575	1.400	160.6	3.294	0.115	7
0.579	1.402	160.6	3.098	0.094	8
0.580	1.403	160.5	3.266	0.078	8
0.585	1.406	160.6	3.219	0.108	7
0.590	1.410	160.5	3.129	0.077	8
0.596	1.414	160.7	2.946	0.086	6
0.596	1.414	160.7	2.961	0.104	7
0.599	1.416	160.6	3.104	0.075	8
0.607	1.421	160.8	3.066	0.098	7

Pion-Lab.-Angle: 150 Degree

k_{lab} [GeV]	W_{CM} [GeV]	Θ_{CM} [deg.]	$d\sigma/d\Omega$ [μb/st]	Error [μb/st]	#
0.609	1.422	160.7	3.154	0.073	8
0.618	1.428	160.9	3.160	0.092	7
0.620	1.430	160.8	3.097	0.073	8
0.631	1.437	160.9	3.135	0.073	8
0.631	1.437	161.0	3.031	0.095	7
0.639	1.442	161.0	3.086	0.093	9
0.643	1.445	161.0	3.059	0.073	8
0.645	1.446	161.1	3.019	0.089	9
0.650	1.449	161.1	3.172	0.089	9
0.655	1.452	161.1	3.089	0.070	8
0.656	1.453	161.2	3.093	0.085	9
0.662	1.457	161.2	3.014	0.087	9
0.667	1.460	161.3	3.085	0.090	9
0.668	1.461	161.1	3.054	0.070	8
0.673	1.464	161.3	3.171	0.090	9
0.679	1.468	161.4	2.996	0.087	9
0.682	1.470	161.3	3.282	0.073	8
0.685	1.472	161.4	3.239	0.086	9
0.692	1.476	161.5	3.105	0.091	9
0.697	1.479	161.3	3.330	0.071	8
0.698	1.480	161.5	3.332	0.090	9
0.705	1.484	161.6	3.598	0.092	9
0.712	1.489	161.6	3.522	0.088	9
0.718	1.493	161.5	3.424	0.108	10
0.719	1.493	161.7	3.588	0.089	9
0.725	1.497	161.6	3.315	0.102	10
0.726	1.498	161.7	3.123	0.084	9
0.731	1.501	161.6	3.056	0.097	10
0.734	1.503	161.8	2.976	0.083	9
0.738	1.505	161.7	3.131	0.099	10
0.742	1.508	161.8	2.783	0.079	9
0.745	1.509	161.7	3.050	0.097	10
0.749	1.512	161.9	2.852	0.081	9
0.753	1.514	161.8	2.901	0.096	10
0.758	1.517	161.9	2.732	0.080	9
0.760	1.519	161.8	2.715	0.094	10
0.767	1.523	162.0	2.692	0.076	9
0.768	1.524	161.9	2.758	0.090	10
0.775	1.528	162.0	2.479	0.078	9
0.776	1.529	161.9	2.633	0.092	10
0.784	1.533	162.1	2.351	0.071	9
0.784	1.533	162.0	2.345	0.088	10
0.793	1.539	162.0	2.486	0.088	10
0.794	1.540	162.2	2.362	0.072	9
0.801	1.544	162.1	2.437	0.089	10
0.803	1.545	162.2	2.148	0.066	9
0.810	1.549	162.2	2.272	0.080	10
0.818	1.554	162.2	2.449	0.077	11
0.819	1.555	162.2	2.481	0.087	10
0.826	1.559	162.3	2.424	0.075	11

Pion-Lab.-Angle: 150 Degree

k_{lab} [GeV]	W_{CM} [GeV]	Θ_{CM} [deg.]	$d\sigma/d\Omega$ [$\mu b/st$]	Error [$\mu b/st$]	#
0.829	1.561	162.3	2.260	0.088	10
0.835	1.564	162.3	2.321	0.072	11
0.839	1.567	162.3	2.266	0.083	10
0.843	1.569	162.4	2.308	0.073	11
0.849	1.573	162.4	2.534	0.082	10
0.852	1.575	162.4	2.363	0.071	11
0.859	1.579	162.5	2.378	0.086	10
0.861	1.580	162.5	2.329	0.074	11
0.870	1.585	162.5	2.377	0.083	10
0.871	1.586	162.5	2.442	0.074	11
0.880	1.591	162.6	2.530	0.074	11
0.882	1.592	162.6	2.357	0.086	10
0.886	1.595	162.6	2.435	0.054	12
0.890	1.597	162.6	2.471	0.071	11
0.894	1.599	162.7	2.295	0.077	10
0.896	1.601	162.7	2.460	0.056	12
0.900	1.603	162.7	2.460	0.075	11
0.906	1.606	162.7	2.431	0.054	12
0.910	1.609	162.8	2.497	0.075	11
0.916	1.612	162.8	2.336	0.054	12
0.921	1.615	162.8	2.465	0.077	11
0.926	1.618	162.9	2.494	0.055	12
0.933	1.622	162.9	2.509	0.074	11
0.937	1.624	162.9	2.449	0.053	12
0.944	1.628	163.0	2.563	0.074	11
0.948	1.631	163.0	2.579	0.055	12
0.956	1.635	163.0	2.598	0.076	11
0.959	1.637	163.1	2.485	0.055	12
0.968	1.642	163.1	2.530	0.072	11
0.971	1.644	163.1	2.440	0.054	12
0.980	1.649	163.2	2.591	0.071	11
0.983	1.651	163.2	2.421	0.053	12
0.994	1.657	163.2	2.523	0.073	11
0.996	1.658	163.3	2.471	0.054	12
1.007	1.664	163.3	2.341	0.068	11
1.007	1.664	163.3	2.473	0.042	13
1.009	1.665	163.3	2.443	0.053	12
1.020	1.672	163.4	2.359	0.042	13
1.021	1.672	163.4	2.310	0.070	11
1.022	1.673	163.4	2.331	0.053	12
1.033	1.679	163.5	2.324	0.041	13
1.035	1.680	163.5	2.187	0.049	12
1.036	1.681	163.5	2.176	0.067	11
1.046	1.686	163.5	2.078	0.039	13
1.050	1.688	163.6	1.952	0.049	12
1.051	1.689	163.5	2.019	0.061	11
1.059	1.693	163.6	1.908	0.038	13
1.064	1.696	163.6	1.893	0.047	12
1.066	1.697	163.6	1.737	0.063	11
1.073	1.701	163.7	1.663	0.037	13

Pion-Lab.-Angle: 150 Degree

k_{lab} [GeV]	W_{CM} [GeV]	Θ_{CM} [deg.]	$d\sigma/d\Omega$ [$\mu b/st$]	Error [$\mu b/st$]	#
1.080	1.705	163.7	1.581	0.044	12
1.083	1.707	163.7	1.544	0.058	11
1.088	1.709	163.7	1.516	0.036	13
1.096	1.714	163.8	1.351	0.041	12
1.103	1.718	163.8	1.344	0.035	13
1.112	1.723	163.8	1.265	0.039	12
1.119	1.726	163.9	1.118	0.033	13
1.123	1.729	164.0	1.170	0.034	14
1.130	1.732	163.9	1.086	0.037	12
1.135	1.735	164.0	1.086	0.032	13
1.139	1.737	164.1	1.087	0.034	14
1.147	1.741	164.0	0.998	0.035	12
1.153	1.745	164.1	0.903	0.031	13
1.154	1.745	164.2	0.997	0.032	14
1.166	1.752	164.1	0.818	0.033	12
1.169	1.753	164.1	0.899	0.030	13
1.170	1.754	164.2	0.876	0.031	14
1.186	1.762	164.3	0.849	0.031	14
1.187	1.763	164.2	0.796	0.028	13
1.204	1.772	164.4	0.794	0.029	14
1.207	1.774	164.3	0.772	0.027	13
1.221	1.781	164.5	0.740	0.029	14
1.226	1.784	164.4	0.729	0.027	13
1.240	1.791	164.6	0.702	0.028	14
1.246	1.794	164.5	0.659	0.025	13
1.260	1.801	164.7	0.703	0.028	14
1.268	1.806	164.5	0.633	0.024	13
1.279	1.811	164.7	0.658	0.027	14
1.280	1.812	164.7	0.638	0.025	15
1.290	1.817	164.6	0.550	0.023	13
1.300	1.822	164.8	0.653	0.024	15
1.300	1.822	164.8	0.641	0.027	14
1.319	1.832	164.9	0.587	0.024	15
1.321	1.833	164.9	0.552	0.025	14
1.339	1.842	165.0	0.594	0.023	15
1.344	1.845	165.0	0.578	0.024	14
1.361	1.853	165.1	0.591	0.022	15
1.366	1.856	165.1	0.551	0.024	14
1.382	1.864	165.1	0.529	0.022	15
1.391	1.868	165.2	0.523	0.023	14
1.405	1.875	165.2	0.513	0.021	15
1.417	1.881	165.3	0.459	0.022	14
1.429	1.887	165.3	0.485	0.021	15
1.442	1.894	165.3	0.420	0.021	14
1.450	1.898	165.4	0.456	0.020	16
1.454	1.900	165.4	0.415	0.020	15
1.474	1.910	165.5	0.413	0.019	16
1.480	1.913	165.5	0.409	0.019	15
1.498	1.921	165.6	0.376	0.018	16
1.506	1.925	165.6	0.350	0.018	15

Pion-Lab.-Angle: 150 Degree

k_{lab} [GeV]	W_{CM} [GeV]	Θ_{CM} [deg.]	$d\sigma/d\Omega$ [$\mu b/st$]	Error [$\mu b/st$]	#
1.525	1.934	165.7	0.338	0.018	16
1.534	1.939	165.7	0.300	0.018	15
1.553	1.948	165.8	0.290	0.017	16
1.564	1.953	165.8	0.269	0.017	15
1.581	1.961	165.9	0.275	0.016	16
1.594	1.968	165.9	0.250	0.016	15
1.610	1.975	166.0	0.217	0.015	16
1.627	1.983	166.0	0.226	0.015	15
1.641	1.990	166.1	0.205	0.015	16
1.674	2.005	166.2	0.177	0.014	16
1.681	2.009	166.2	0.162	0.015	17
1.707	2.021	166.3	0.155	0.013	16
1.711	2.023	166.3	0.142	0.014	17
1.743	2.037	166.4	0.142	0.013	17
1.744	2.038	166.4	0.129	0.012	16
1.777	2.053	166.5	0.111	0.013	17
1.780	2.054	166.5	0.123	0.012	16
1.813	2.069	166.6	0.102	0.012	17
1.821	2.073	166.6	0.118	0.011	16
1.850	2.086	166.7	0.101	0.011	17
1.888	2.103	166.8	0.083	0.011	17
1.928	2.121	166.9	0.073	0.010	17
1.970	2.139	167.0	0.057	0.010	17
2.016	2.160	167.1	0.054	0.009	17
2.062	2.179	167.2	0.051	0.009	17
2.112	2.201	167.4	0.054	0.008	17

Pion-Lab.-Angle: 135 Degree

k_{lab} [GeV]	W_{CM} [GeV]	Θ_{CM} [deg.]	$d\sigma/d\Omega$ [$\mu b/st$]	Error [$\mu b/st$]	#
0.303	1.204	146.6	17.622	0.566	1
0.311	1.210	146.7	18.041	0.552	1
0.320	1.217	146.8	18.460	0.546	1
0.330	1.225	146.9	16.528	0.407	2
0.330	1.225	146.9	16.261	0.501	1
0.338	1.231	147.0	14.345	0.372	2
0.346	1.237	147.2	12.956	0.345	2
0.356	1.244	147.3	11.147	0.315	2
0.359	1.247	147.3	10.355	0.254	3
0.367	1.253	147.4	8.903	0.231	3

Pion-Lab.-Angle: 135 Degree

k_{lab} [GeV]	W_{CM} [GeV]	Θ_{CM} [deg.]	$d\sigma/d\Omega$ [$\mu b/st$]	Error [$\mu b/st$]	#
0.375	1.259	147.6	8.288	0.216	3
0.383	1.265	147.7	7.344	0.202	3
0.393	1.272	147.8	5.997	0.187	3
0.403	1.279	147.9	5.493	0.151	4
0.403	1.279	147.9	5.446	0.165	3
0.410	1.284	148.0	4.965	0.141	4
0.417	1.290	148.2	4.705	0.141	4
0.425	1.295	148.3	4.669	0.137	4
0.433	1.301	148.4	4.367	0.134	4
0.442	1.308	148.5	4.146	0.128	4
0.451	1.314	148.6	3.867	0.119	4
0.453	1.315	148.6	3.926	0.119	5
0.458	1.319	148.7	3.637	0.122	5
0.462	1.322	148.8	3.843	0.116	4
0.464	1.323	148.8	3.363	0.118	5
0.470	1.328	148.9	3.528	0.117	5
0.477	1.332	149.0	3.456	0.114	5
0.483	1.337	149.1	3.570	0.113	5
0.490	1.342	149.2	3.790	0.118	5
0.497	1.346	149.2	3.339	0.110	5
0.505	1.352	149.3	3.214	0.108	5
0.513	1.358	149.5	3.293	0.109	5
0.521	1.363	149.6	3.138	0.107	5
0.526	1.367	149.6	3.525	0.104	6
0.530	1.369	149.7	2.999	0.103	5
0.534	1.372	149.7	3.557	0.105	6
0.542	1.377	149.8	3.116	0.098	6
0.550	1.383	149.9	3.451	0.102	6
0.558	1.388	150.0	3.417	0.101	6
0.567	1.394	150.2	3.416	0.100	6
0.576	1.400	150.3	3.216	0.096	6
0.585	1.406	150.4	3.105	0.095	6
0.596	1.414	150.5	2.988	0.091	6
0.606	1.420	150.6	3.154	0.093	6
0.612	1.424	150.7	3.393	0.097	7
0.617	1.428	150.7	3.311	0.096	7
0.618	1.428	150.8	3.131	0.091	6
0.621	1.430	150.8	3.176	0.095	7
0.626	1.434	150.9	3.072	0.093	7
0.630	1.436	150.9	2.878	0.087	6
0.632	1.437	151.0	3.276	0.095	7
0.636	1.440	151.0	2.936	0.089	7
0.642	1.444	151.0	3.236	0.094	7
0.647	1.447	151.1	3.269	0.094	7
0.653	1.451	151.2	3.168	0.093	7
0.659	1.455	151.3	3.402	0.094	7
0.664	1.458	151.3	3.492	0.096	7
0.670	1.462	151.4	3.330	0.094	7
0.672	1.463	151.4	3.217	0.109	8
0.677	1.467	151.4	3.309	0.092	7

Pion-Lab.-Angle: 135 Degree

k_{lab} [GeV]	W_{CM} [GeV]	Θ_{CM} [deg.]	$d\sigma/d\Omega$ [$\mu b/st$]	Error [$\mu b/st$]	#
0.678	1.467	151.4	3.321	0.107	8
0.683	1.470	151.5	3.529	0.096	7
0.684	1.471	151.5	3.552	0.105	8
0.689	1.474	151.6	3.563	0.094	7
0.689	1.474	151.6	3.519	0.109	8
0.696	1.479	151.6	3.641	0.096	7
0.696	1.479	151.6	3.559	0.112	8
0.702	1.482	151.7	3.755	0.112	8
0.702	1.482	151.7	3.626	0.095	7
0.708	1.486	151.8	3.871	0.110	8
0.710	1.488	151.8	3.835	0.098	7
0.714	1.490	151.8	3.889	0.111	8
0.717	1.492	151.9	3.835	0.098	7
0.721	1.494	151.9	3.904	0.110	8
0.724	1.496	152.0	3.758	0.096	7
0.728	1.499	152.0	3.733	0.105	8
0.732	1.501	152.0	3.514	0.093	7
0.734	1.503	152.0	3.496	0.105	8
0.739	1.506	152.1	3.329	0.090	7
0.742	1.508	152.1	3.295	0.103	8
0.748	1.511	152.2	3.293	0.090	7
0.749	1.512	152.2	3.335	0.102	8
0.756	1.516	152.3	3.039	0.087	7
0.756	1.516	152.3	3.046	0.098	8
0.764	1.521	152.4	2.876	0.103	8
0.772	1.526	152.5	2.818	0.091	8
0.780	1.531	152.5	2.592	0.090	8
0.788	1.536	152.6	2.730	0.093	8
0.790	1.537	152.6	2.693	0.092	9
0.797	1.541	152.7	2.511	0.085	8
0.798	1.542	152.7	2.580	0.088	9
0.805	1.546	152.8	2.551	0.089	9
0.806	1.547	152.8	2.541	0.083	8
0.813	1.551	152.9	2.690	0.088	9
0.815	1.552	152.9	2.552	0.085	8
0.821	1.556	152.9	2.371	0.083	9
0.825	1.558	153.0	2.312	0.082	8
0.829	1.561	153.0	2.207	0.083	9
0.835	1.564	153.1	2.414	0.079	8
0.837	1.566	153.1	2.367	0.089	9
0.844	1.570	153.1	2.463	0.080	8
0.846	1.571	153.2	2.454	0.080	9
0.854	1.576	153.3	2.296	0.086	9
0.864	1.582	153.4	2.415	0.087	9
0.873	1.587	153.4	2.506	0.084	9
0.883	1.593	153.5	2.482	0.082	9
0.892	1.598	153.6	2.414	0.088	9
0.903	1.605	153.7	2.410	0.082	9
0.910	1.609	153.7	2.434	0.058	10
0.913	1.610	153.8	2.401	0.083	9

Pion-Lab.-Angle: 135 Degree

k_{lab} [GeV]	W_{CM} [GeV]	Θ_{CM} [deg.]	$d\sigma/d\Omega$ [$\mu b/st$]	Error [$\mu b/st$]	#
0.919	1.614	153.8	2.293	0.058	10
0.924	1.617	153.9	2.412	0.081	9
0.930	1.620	153.9	2.493	0.059	10
0.935	1.623	154.0	2.424	0.082	9
0.940	1.626	154.0	2.488	0.059	10
0.947	1.630	154.1	2.495	0.081	9
0.951	1.632	154.1	2.545	0.059	10
0.958	1.636	152.2	2.592	0.082	9
0.962	1.639	154.2	2.632	0.059	10
0.970	1.643	154.3	2.753	0.088	9
0.973	1.645	154.3	2.646	0.059	10
0.983	1.651	154.4	2.727	0.085	9
0.985	1.652	154.4	2.635	0.059	10
0.988	1.654	154.4	2.505	0.061	11
0.996	1.658	154.5	2.467	0.059	10
0.996	1.658	154.5	2.590	0.084	9
0.999	1.660	154.5	2.638	0.063	11
1.008	1.665	154.6	2.664	0.059	10
1.010	1.666	154.6	2.507	0.080	9
1.011	1.667	154.6	2.670	0.064	11
1.021	1.672	154.7	2.539	0.060	10
1.023	1.673	154.7	2.641	0.063	11
1.024	1.674	154.7	2.466	0.079	9
1.035	1.680	154.8	2.470	0.057	10
1.035	1.680	154.8	2.458	0.061	11
1.048	1.687	154.9	2.372	0.062	11
1.048	1.687	154.9	2.143	0.053	10
1.061	1.695	155.0	2.260	0.057	11
1.062	1.695	155.0	2.150	0.054	10
1.075	1.702	155.1	2.012	0.056	11
1.076	1.703	155.1	1.924	0.052	10
1.089	1.710	155.2	1.891	0.055	11
1.092	1.712	155.2	1.745	0.049	10
1.103	1.718	155.3	1.588	0.050	11
1.107	1.720	155.3	1.534	0.046	10
1.118	1.726	155.4	1.472	0.048	11
1.124	1.729	155.5	1.340	0.044	10
1.134	1.734	155.5	1.296	0.046	11
1.140	1.738	155.6	1.280	0.042	10
1.150	1.743	155.6	1.226	0.044	11
1.159	1.748	155.7	1.110	0.040	10
1.168	1.753	155.8	1.113	0.042	11
1.184	1.761	155.9	1.027	0.041	11
1.202	1.771	156.0	0.998	0.040	11
1.221	1.781	156.1	0.901	0.038	11
1.239	1.790	156.3	0.982	0.032	12
1.241	1.791	156.3	0.922	0.039	11
1.257	1.800	156.4	0.995	0.032	12
1.261	1.802	156.4	0.897	0.037	11
1.274	1.809	156.5	0.944	0.031	12

Pion-Lab.-Angle: 135 Degree

k_{lab} [GeV]	W_{CM} [GeV]	Θ_{CM} [deg.]	$d\sigma/d\Omega$ [$\mu b/st$]	Error [$\mu b/st$]	#
1.293	1.818	156.6	0.939	0.030	12
1.313	1.829	156.7	0.917	0.030	12
1.333	1.839	156.9	0.890	0.029	12
1.353	1.849	157.0	0.901	0.029	12
1.375	1.860	157.1	0.827	0.028	12
1.397	1.871	157.2	0.777	0.028	12
1.421	1.883	157.4	0.791	0.027	12
1.445	1.895	157.5	0.720	0.026	12
1.462	1.904	157.6	0.700	0.023	13
1.470	1.908	157.6	0.636	0.025	12
1.485	1.915	157.7	0.606	0.022	13
1.498	1.921	157.8	0.594	0.024	12
1.510	1.927	157.9	0.575	0.022	13
1.525	1.934	157.9	0.513	0.022	12
1.536	1.940	158.0	0.528	0.021	13
1.555	1.949	158.1	0.468	0.022	12
1.561	1.952	158.1	0.476	0.020	13
1.585	1.963	158.2	0.378	0.021	12
1.589	1.965	158.3	0.413	0.019	13
1.618	1.979	158.4	0.386	0.018	13
1.647	1.993	158.5	0.338	0.017	13
1.680	2.008	158.7	0.289	0.016	13
1.701	2.018	158.8	0.283	0.015	14
1.711	2.023	158.9	0.240	0.016	13
1.733	2.033	159.0	0.257	0.014	14
1.746	2.039	159.0	0.225	0.015	13
1.764	2.047	159.1	0.231	0.014	14
1.781	2.055	159.2	0.195	0.014	13
1.797	2.062	159.2	0.196	0.013	14
1.833	2.078	159.4	0.169	0.012	14
1.870	2.095	159.6	0.141	0.012	14
1.910	2.113	159.7	0.104	0.011	14
1.952	2.132	159.9	0.080	0.010	14
1.993	2.150	160.1	0.078	0.010	14
2.039	2.169	160.2	0.061	0.009	14

Pion-Lab.-Angle: 120 Degree

k_{lab} [GeV]	W_{CM} [GeV]	Θ_{CM} [deg.]	$d\sigma/d\Omega$ [$\mu b/st$]	Error [$\mu b/st$]	#
0.311	1.210	134.4	20.197	0.554	1
0.316	1.214	134.5	19.471	0.535	1
0.322	1.218	134.6	18.609	0.521	1
0.328	1.223	134.7	17.195	0.495	1
0.335	1.228	134.8	15.429	0.470	1
0.337	1.230	134.9	15.347	0.347	2
0.342	1.234	135.0	14.882	0.447	1
0.343	1.235	135.0	14.974	0.337	2
0.350	1.240	135.1	14.458	0.326	2
0.357	1.245	135.2	12.429	0.299	2
0.365	1.251	135.4	11.117	0.277	2
0.374	1.258	135.5	9.436	0.251	2
0.375	1.259	135.6	9.205	0.260	3
0.383	1.265	135.7	8.388	0.240	3
0.392	1.271	135.9	7.853	0.224	3
0.401	1.278	136.0	6.567	0.214	3
0.411	1.285	136.2	5.861	0.188	3
0.416	1.289	136.3	6.005	0.155	4
0.420	1.292	136.4	5.579	0.147	4
0.422	1.293	136.4	5.120	0.184	3
0.425	1.295	136.5	5.434	0.146	4
0.430	1.299	136.6	5.156	0.139	4
0.435	1.303	136.7	5.116	0.138	4
0.441	1.307	136.8	4.808	0.136	4
0.446	1.310	136.9	4.749	0.131	4
0.451	1.314	137.0	4.110	0.136	5
0.453	1.315	137.0	4.490	0.128	4
0.457	1.318	137.1	4.215	0.127	5
0.459	1.320	137.1	4.370	0.125	4
0.462	1.322	137.2	3.935	0.121	5
0.465	1.324	137.2	4.232	0.121	4
0.468	1.326	137.3	4.057	0.122	5
0.472	1.329	137.4	4.199	0.120	4
0.474	1.330	137.4	3.968	0.118	5
0.479	1.334	137.5	4.040	0.117	4
0.480	1.335	137.5	3.900	0.115	5
0.487	1.339	137.6	3.887	0.111	5
0.494	1.344	137.7	3.557	0.119	5
0.501	1.349	137.8	3.441	0.103	5
0.508	1.354	138.0	3.515	0.106	5
0.516	1.360	138.1	3.495	0.105	5
0.517	1.360	138.1	3.807	0.109	6
0.524	1.365	138.2	3.669	0.104	6
0.524	1.365	138.2	3.455	0.107	5
0.531	1.370	138.4	3.581	0.103	6
0.538	1.375	138.5	3.465	0.101	6
0.546	1.380	138.6	3.497	0.101	6
0.554	1.386	138.8	3.645	0.101	6
0.562	1.391	138.9	3.566	0.099	6
0.571	1.397	139.0	3.316	0.097	6

Pion-Lab.-Angle: 120 Degree

k_{lab} [GeV]	W_{CM} [GeV]	Θ_{CM} [deg.]	$d\sigma/d\Omega$ [$\mu b/st$]	Error [$\mu b/st$]	#
0.580	1.403	139.2	3.473	0.096	6
0.590	1.410	139.3	3.431	0.096	6
0.594	1.412	139.4	3.331	0.119	7
0.598	1.415	139.5	3.533	0.118	7
0.600	1.416	139.5	3.454	0.095	6
0.602	1.418	139.6	3.225	0.115	7
0.607	1.421	139.6	3.375	0.116	7
0.611	1.424	139.7	3.469	0.094	6
0.612	1.424	139.7	3.493	0.112	7
0.616	1.427	139.8	3.294	0.111	7
0.621	1.430	139.8	3.240	0.111	7
0.624	1.432	139.9	3.283	0.108	8
0.626	1.434	139.9	3.365	0.114	7
0.629	1.436	140.0	3.514	0.109	8
0.631	1.437	140.0	3.246	0.110	7
0.633	1.438	140.0	3.393	0.108	8
0.636	1.440	140.1	3.289	0.118	7
0.638	1.441	140.1	3.601	0.111	8
0.641	1.443	140.2	3.420	0.116	7
0.643	1.445	140.2	3.468	0.109	8
0.646	1.447	140.2	3.456	0.112	7
0.649	1.449	140.3	3.553	0.109	8
0.652	1.450	140.3	3.714	0.116	7
0.653	1.451	140.4	3.661	0.110	8
0.657	1.454	140.4	3.605	0.112	7
0.659	1.455	140.4	3.690	0.110	8
0.663	1.458	140.5	3.598	0.116	7
0.664	1.458	140.5	3.631	0.110	8
0.669	1.461	140.6	3.635	0.116	7
0.670	1.462	140.6	3.569	0.110	8
0.675	1.465	140.6	3.708	0.117	7
0.675	1.465	140.7	3.707	0.111	8
0.681	1.469	140.7	3.883	0.122	7
0.681	1.469	140.8	3.907	0.113	8
0.687	1.473	140.8	3.911	0.111	8
0.687	1.473	140.8	3.984	0.118	7
0.693	1.477	140.9	3.866	0.112	8
0.694	1.477	140.9	4.156	0.122	7
0.700	1.481	141.0	4.285	0.116	8
0.700	1.481	141.0	4.222	0.121	7
0.705	1.484	141.1	4.433	0.109	9
0.706	1.485	141.1	4.261	0.115	8
0.708	1.486	141.1	4.218	0.116	7
0.711	1.488	141.2	4.594	0.109	9
0.712	1.489	141.2	4.205	0.114	8
0.715	1.491	141.2	4.120	0.120	7
0.717	1.492	141.3	4.313	0.110	9
0.719	1.493	141.3	4.536	0.119	8
0.722	1.495	141.4	4.161	0.118	7
0.723	1.496	141.4	4.537	0.109	9

Pion-Lab.-Angle: 120 Degree

k_{lab} [GeV]	W_{CM} [GeV]	Θ_{CM} [deg.]	$d\sigma/d\Omega$ [$\mu b/st$]	Error [$\mu b/st$]	#
0.727	1.498	141.4	4.132	0.113	8
0.729	1.499	141.4	4.166	0.107	9
0.734	1.503	141.5	4.069	0.110	8
0.735	1.503	141.5	4.060	0.101	9
0.741	1.507	141.6	4.173	0.113	8
0.742	1.508	141.6	4.025	0.101	9
0.748	1.511	141.7	3.715	0.106	8
0.748	1.511	141.7	3.928	0.101	9
0.755	1.516	141.8	3.702	0.097	9
0.756	1.516	141.8	3.636	0.105	8
0.762	1.520	141.9	3.696	0.096	9
0.764	1.521	141.9	3.477	0.101	8
0.769	1.524	142.0	3.462	0.096	9
0.776	1.529	142.1	3.369	0.092	9
0.784	1.533	142.2	3.412	0.091	9
0.791	1.538	142.3	3.132	0.089	9
0.800	1.543	142.4	2.998	0.088	9
0.807	1.547	142.5	3.006	0.084	9
0.816	1.553	142.6	2.646	0.082	9
0.824	1.558	142.7	2.817	0.083	9
0.833	1.563	142.8	2.685	0.082	9
0.842	1.569	142.9	2.563	0.080	9
0.851	1.574	143.0	2.555	0.077	9
0.861	1.580	143.2	2.641	0.078	9
0.868	1.584	143.3	2.618	0.074	10
0.871	1.586	143.3	2.469	0.075	9
0.876	1.589	143.3	2.497	0.078	10
0.881	1.592	143.4	2.506	0.076	9
0.884	1.594	143.5	2.567	0.076	10
0.893	1.599	143.6	2.622	0.076	10
0.903	1.605	143.7	2.778	0.078	10
0.911	1.609	143.8	2.680	0.076	10
0.921	1.615	143.9	2.739	0.075	10
0.930	1.620	144.0	2.795	0.078	10
0.940	1.626	144.1	2.871	0.078	10
0.950	1.632	144.2	2.942	0.079	10
0.961	1.638	144.4	2.901	0.079	10
0.972	1.645	144.5	3.074	0.079	10
0.983	1.651	144.6	3.067	0.078	10
0.994	1.657	144.7	3.194	0.079	10
1.007	1.664	144.9	3.032	0.078	10
1.018	1.671	145.0	3.029	0.078	10
1.031	1.678	145.1	2.890	0.076	10
1.044	1.685	145.2	2.870	0.075	10
1.058	1.693	145.4	2.688	0.073	10
1.062	1.695	145.5	2.594	0.064	11
1.072	1.701	145.5	2.490	0.070	10
1.073	1.701	145.5	2.381	0.061	11
1.085	1.708	145.7	2.296	0.060	11
1.086	1.708	145.7	2.234	0.067	10

Pion-Lab.-Angle: 120 Degree

k_{lab} [GeV]	W_{CM} [GeV]	Θ_{CM} [deg.]	$d\sigma/d\Omega$ [$\mu b/st$]	Error [$\mu b/st$]	#
1.098	1.715	145.8	1.916	0.057	11
1.102	1.717	145.8	1.794	0.060	10
1.112	1.723	146.0	1.857	0.054	11
1.125	1.730	146.1	1.677	0.053	11
1.139	1.737	146.2	1.501	0.050	11
1.154	1.745	146.4	1.359	0.047	11
1.167	1.752	146.5	1.294	0.046	11
1.183	1.761	146.6	1.171	0.045	11
1.200	1.770	146.8	1.105	0.043	11
1.216	1.778	146.9	1.123	0.042	11
1.233	1.787	147.1	1.073	0.041	11
1.250	1.796	147.2	1.059	0.041	11
1.261	1.802	147.3	1.123	0.034	12
1.268	1.806	147.4	1.070	0.041	11
1.279	1.811	147.5	1.092	0.033	12
1.287	1.815	147.5	1.082	0.040	11
1.296	1.820	147.6	1.090	0.032	12
1.314	1.829	147.8	1.157	0.033	12
1.332	1.838	147.9	1.066	0.032	12
1.353	1.849	148.1	1.044	0.032	12
1.371	1.858	148.2	1.019	0.031	12
1.393	1.869	148.4	0.960	0.029	12
1.413	1.879	148.6	0.924	0.030	12
1.437	1.891	148.8	0.918	0.029	12
1.459	1.902	148.9	0.832	0.028	12
1.484	1.914	149.1	0.774	0.027	12
1.506	1.925	149.3	0.784	0.022	13
1.507	1.926	149.3	0.693	0.026	12
1.529	1.936	149.4	0.712	0.021	13
1.536	1.940	149.5	0.631	0.024	12
1.552	1.948	149.6	0.648	0.020	13
1.562	1.952	149.6	0.589	0.022	12
1.578	1.960	149.8	0.600	0.020	13
1.604	1.972	150.0	0.511	0.019	13
1.632	1.986	150.1	0.461	0.018	13
1.659	1.998	150.3	0.411	0.017	13
1.689	2.012	150.5	0.394	0.017	13
1.720	2.027	150.7	0.354	0.016	13
1.749	2.040	150.9	0.324	0.015	13
1.764	2.047	151.0	0.299	0.013	14
1.785	2.057	151.1	0.256	0.014	13
1.796	2.062	151.2	0.264	0.013	14
1.827	2.076	151.4	0.246	0.012	14
1.858	2.090	151.5	0.207	0.012	14
1.893	2.105	151.7	0.184	0.011	14
1.927	2.120	151.9	0.139	0.011	14
1.965	2.137	152.1	0.125	0.010	14
2.005	2.155	152.4	0.099	0.009	14
2.046	2.173	152.6	0.073	0.009	14
2.090	2.191	152.8	0.086	0.008	14

Pion-Lab.-Angle: 105 Degree

k_{lab} [GeV]	W_{CM} [GeV]	Θ_{CM} [deg.]	$d\sigma/d\Omega$ [$\mu b/st$]	Error [$\mu b/st$]	#
0.322	1.218	121.7	20.473	0.584	1
0.328	1.223	121.8	18.889	0.536	1
0.334	1.228	121.9	18.965	0.548	1
0.340	1.232	122.1	16.969	0.506	1
0.347	1.238	122.2	15.425	0.369	2
0.348	1.238	122.3	14.865	0.472	1
0.353	1.242	122.4	14.470	0.350	2
0.355	1.244	122.4	13.360	0.447	1
0.360	1.247	122.5	12.619	0.332	2
0.368	1.253	122.7	11.718	0.308	2
0.376	1.259	122.9	10.968	0.293	2
0.377	1.260	122.9	10.828	0.244	3
0.383	1.265	123.0	9.314	0.230	3
0.385	1.266	123.1	9.104	0.264	2
0.389	1.269	123.2	8.809	0.216	3
0.396	1.274	123.3	7.961	0.209	3
0.402	1.279	123.5	8.052	0.208	3
0.409	1.284	123.6	6.722	0.188	3
0.417	1.290	123.8	6.502	0.182	3
0.419	1.291	123.8	6.672	0.183	4
0.423	1.294	123.9	6.615	0.180	4
0.425	1.295	124.0	5.757	0.170	3
0.428	1.298	124.0	6.079	0.174	4
0.433	1.301	124.2	5.643	0.166	4
0.438	1.305	124.3	5.468	0.166	4
0.443	1.308	124.4	5.291	0.166	4
0.449	1.313	124.5	5.268	0.158	4
0.454	1.316	124.6	4.965	0.160	4
0.460	1.320	124.7	4.702	0.154	4
0.466	1.325	124.9	4.703	0.150	4
0.472	1.329	125.0	4.600	0.141	5
0.473	1.330	125.0	4.314	0.140	4
0.478	1.333	125.1	4.373	0.141	5
0.480	1.335	125.2	4.566	0.141	4
0.483	1.337	125.3	4.166	0.140	5
0.490	1.342	125.4	4.409	0.144	5
0.496	1.346	125.5	4.377	0.140	5
0.502	1.350	125.7	3.940	0.135	5
0.509	1.355	125.8	3.994	0.132	5
0.516	1.360	125.9	3.915	0.131	5
0.523	1.364	126.1	3.700	0.124	5
0.531	1.370	126.3	3.920	0.124	5
0.532	1.371	126.3	3.978	0.115	6
0.539	1.375	126.4	4.049	0.114	6
0.539	1.375	126.4	3.672	0.120	5
0.546	1.380	126.6	3.693	0.110	6
0.548	1.382	126.6	3.758	0.125	5
0.553	1.385	126.7	3.727	0.110	6
0.561	1.390	126.9	3.756	0.105	6
0.569	1.396	127.0	3.867	0.108	6

Pion-Lab.-Angle: 105 Degree

k_{lab} [GeV]	W_{CM} [GeV]	Θ_{CM} [deg.]	$d\sigma/d\Omega$ [$\mu b/st$]	Error [$\mu b/st$]	#
0.577	1.401	127.2	3.746	0.106	6
0.586	1.407	127.4	3.812	0.104	6
0.595	1.413	127.5	3.602	0.101	6
0.600	1.416	127.7	4.104	0.120	7
0.604	1.419	127.7	3.707	0.115	7
0.605	1.420	127.7	3.746	0.102	6
0.608	1.422	127.8	3.770	0.118	7
0.612	1.424	127.9	3.817	0.120	7
0.615	1.426	127.9	3.572	0.100	6
0.617	1.428	128.0	3.916	0.119	7
0.621	1.430	128.0	3.625	0.113	7
0.625	1.433	128.1	3.458	0.098	6
0.626	1.434	128.1	3.751	0.117	7
0.631	1.437	128.3	3.914	0.117	7
0.635	1.439	128.3	3.818	0.117	7
0.640	1.443	128.4	3.945	0.117	7
0.645	1.446	128.5	4.058	0.120	7
0.650	1.449	128.6	3.957	0.118	7
0.655	1.452	128.7	4.290	0.120	7
0.657	1.454	128.7	4.182	0.137	8
0.660	1.456	128.8	4.528	0.123	7
0.661	1.456	128.8	4.303	0.139	8
0.666	1.460	128.9	4.215	0.119	7
0.666	1.460	128.9	4.324	0.136	8
0.671	1.463	129.0	4.397	0.136	8
0.671	1.463	129.0	4.517	0.123	7
0.676	1.466	129.1	4.531	0.138	8
0.677	1.467	129.1	4.274	0.119	7
0.681	1.469	129.2	4.133	0.134	8
0.683	1.470	129.2	4.494	0.122	7
0.687	1.473	129.3	4.574	0.143	8
0.689	1.474	129.3	4.686	0.125	7
0.692	1.476	129.4	4.739	0.140	8
0.695	1.478	129.4	4.779	0.123	7
0.697	1.479	129.5	4.929	0.144	8
0.701	1.482	129.5	4.806	0.127	7
0.703	1.483	129.6	5.145	0.144	8
0.705	1.484	129.6	4.872	0.122	9
0.708	1.486	129.6	5.198	0.129	7
0.709	1.487	129.6	5.056	0.148	8
0.711	1.488	129.7	5.045	0.125	9
0.714	1.490	129.7	5.225	0.147	8
0.715	1.491	129.8	5.194	0.126	7
0.716	1.491	129.8	5.048	0.126	9
0.721	1.494	129.9	5.308	0.146	8
0.721	1.494	129.9	5.086	0.125	7
0.722	1.495	129.9	5.081	0.124	9
0.727	1.498	130.0	4.990	0.142	8
0.727	1.498	130.0	5.051	0.124	9
0.733	1.502	130.1	4.805	0.122	9

Pion-Lab.-Angle: 105 Degree

k_{lab} [GeV]	W_{CM} [GeV]	Θ_{CM} [deg.]	$d\sigma/d\Omega$ [$\mu b/st$]	Error [$\mu b/st$]	#
0.733	1.502	130.1	4.984	0.142	8
0.739	1.506	130.2	4.811	0.122	9
0.740	1.506	130.2	4.862	0.142	8
0.745	1.509	130.3	4.616	0.120	9
0.746	1.510	130.3	4.584	0.135	8
0.751	1.513	130.4	4.578	0.116	9
0.753	1.514	130.4	4.796	0.136	8
0.758	1.517	130.5	4.646	0.117	9
0.761	1.519	130.6	4.514	0.133	8
0.764	1.521	130.6	4.451	0.116	9
0.768	1.524	130.7	4.260	0.128	8
0.771	1.526	130.7	4.270	0.113	9
0.775	1.528	130.8	4.011	0.127	8
0.776	1.529	130.8	4.380	0.107	10
0.778	1.530	130.8	4.365	0.111	9
0.782	1.532	130.9	4.094	0.104	10
0.782	1.532	130.9	4.024	0.124	8
0.785	1.534	131.0	3.918	0.108	9
0.788	1.536	131.0	4.034	0.102	10
0.790	1.537	131.0	3.732	0.123	8
0.792	1.538	131.1	3.814	0.106	9
0.795	1.540	131.1	3.837	0.101	10
0.798	1.542	131.1	3.239	0.111	8
0.799	1.543	131.2	3.777	0.104	9
0.802	1.544	131.3	3.458	0.094	10
0.806	1.547	131.3	3.188	0.098	9
0.809	1.549	131.4	3.244	0.092	10
0.814	1.552	131.4	3.314	0.098	9
0.815	1.552	131.5	3.333	0.091	10
0.822	1.557	131.5	3.224	0.099	9
0.823	1.557	131.6	3.115	0.090	10
0.828	1.560	131.6	3.197	0.100	11
0.830	1.561	131.7	3.139	0.088	10
0.831	1.562	131.7	3.052	0.095	9
0.836	1.565	131.8	3.188	0.100	11
0.837	1.566	131.8	3.023	0.086	10
0.839	1.567	131.8	2.992	0.094	9
0.843	1.569	131.9	3.197	0.099	11
0.845	1.570	131.9	3.083	0.087	10
0.848	1.572	132.0	2.908	0.090	9
0.851	1.574	132.0	3.055	0.097	11
0.853	1.575	132.0	2.942	0.087	10
0.856	1.577	132.1	2.781	0.088	9
0.858	1.578	132.1	3.095	0.095	11
0.861	1.580	132.2	2.964	0.086	10
0.866	1.583	132.2	2.715	0.087	9
0.866	1.583	132.3	3.016	0.095	11
0.869	1.585	132.3	2.816	0.081	10
0.873	1.587	132.3	2.950	0.094	11
0.878	1.590	132.4	2.924	0.083	10

Pion-Lab.-Angle: 105 Degree

k_{lab} [GeV]	W_{CM} [GeV]	Θ_{CM} [deg.]	$d\sigma/d\Omega$ [$\mu b/st$]	Error [$\mu b/st$]	#
0.882	1.592	132.5	2.961	0.095	11
0.887	1.595	132.6	2.774	0.081	10
0.890	1.597	132.6	2.908	0.093	11
0.895	1.600	132.6	2.790	0.082	10
0.898	1.602	132.7	3.124	0.095	11
0.905	1.606	132.8	2.864	0.082	10
0.907	1.607	132.8	2.777	0.090	11
0.914	1.611	133.0	2.914	0.082	10
0.916	1.612	133.0	3.149	0.095	11
0.924	1.617	133.1	3.092	0.082	10
0.925	1.617	133.1	2.979	0.093	11
0.934	1.623	133.2	2.962	0.084	10
0.935	1.623	133.3	3.311	0.096	11
0.944	1.628	133.4	3.121	0.094	11
0.944	1.628	133.4	3.057	0.083	10
0.954	1.634	133.5	3.138	0.092	11
0.955	1.635	133.5	3.038	0.084	10
0.964	1.640	133.6	3.388	0.098	11
0.966	1.641	133.7	3.017	0.081	10
0.975	1.646	133.8	3.421	0.095	11
0.986	1.652	133.9	3.386	0.096	11
0.993	1.656	134.1	3.407	0.060	12
0.997	1.659	134.1	3.465	0.096	11
1.003	1.662	134.2	3.469	0.059	12
1.008	1.665	134.3	3.419	0.096	11
1.012	1.667	134.3	3.326	0.058	12
1.021	1.672	134.4	3.596	0.095	11
1.023	1.673	134.5	3.431	0.058	12
1.032	1.678	134.5	3.262	0.090	11
1.033	1.679	134.6	3.231	0.058	12
1.044	1.685	134.8	3.150	0.056	12
1.055	1.691	134.9	2.948	0.055	12
1.066	1.697	135.0	2.643	0.052	12
1.077	1.703	135.1	2.444	0.051	12
1.089	1.710	135.3	2.282	0.048	12
1.101	1.717	135.4	2.005	0.046	12
1.115	1.724	135.6	1.751	0.043	12
1.128	1.731	135.8	1.506	0.040	12
1.141	1.738	135.9	1.259	0.038	12
1.155	1.746	136.1	1.207	0.037	12
1.169	1.753	136.3	1.053	0.034	12
1.178	1.758	136.4	1.088	0.035	13
1.183	1.761	136.4	1.044	0.033	12
1.192	1.766	136.6	0.979	0.033	13
1.199	1.769	136.6	0.896	0.032	12
1.204	1.772	136.7	0.943	0.033	13
1.214	1.777	136.8	0.881	0.031	12
1.218	1.779	136.8	0.992	0.033	13
1.230	1.786	137.0	0.846	0.030	12
1.232	1.787	137.0	0.943	0.031	13

Pion-Lab.-Angle: 105 Degree

k_{lab} [GeV]	W_{CM} [GeV]	Θ_{CM} [deg.]	$d\sigma/d\Omega$ [$\mu b/st$]	Error [$\mu b/st$]	#
1.248	1.795	137.2	0.866	0.032	13
1.248	1.795	137.2	0.782	0.029	12
1.263	1.803	137.4	0.924	0.031	13
1.279	1.811	137.5	0.862	0.030	13
1.294	1.819	137.7	0.912	0.030	13
1.311	1.828	137.9	0.843	0.029	13
1.329	1.837	138.1	0.841	0.028	13
1.346	1.846	138.2	0.874	0.029	13
1.366	1.856	138.4	0.871	0.029	13
1.383	1.864	138.6	0.873	0.028	13
1.387	1.866	138.6	0.845	0.025	14
1.403	1.874	138.8	0.848	0.027	13
1.406	1.876	138.8	0.888	0.025	14
1.423	1.884	139.0	0.870	0.025	14
1.425	1.885	139.0	0.770	0.028	13
1.442	1.894	139.2	0.838	0.024	14
1.446	1.896	139.2	0.760	0.026	13
1.463	1.904	139.4	0.781	0.023	14
1.468	1.907	139.4	0.715	0.025	13
1.482	1.913	139.5	0.778	0.023	14
1.503	1.924	139.8	0.723	0.022	14
1.523	1.933	139.9	0.686	0.022	14
1.545	1.944	140.1	0.669	0.021	14
1.569	1.956	140.4	0.604	0.021	14
1.591	1.966	140.5	0.562	0.020	14
1.599	1.970	140.6	0.567	0.015	15
1.616	1.978	140.7	0.519	0.019	14
1.622	1.981	140.8	0.537	0.015	15
1.642	1.990	141.0	0.474	0.018	14
1.646	1.992	141.0	0.501	0.014	15
1.671	2.004	141.2	0.463	0.014	15
1.695	2.015	141.4	0.405	0.013	15
1.722	2.028	141.6	0.362	0.012	15
1.748	2.040	141.8	0.313	0.012	15
1.778	2.054	142.1	0.306	0.011	15
1.805	2.066	142.3	0.253	0.010	16
1.807	2.067	142.3	0.259	0.011	15
1.836	2.080	142.5	0.209	0.010	15
1.836	2.080	142.5	0.229	0.009	16
1.864	2.092	142.7	0.195	0.009	16
1.871	2.096	142.8	0.200	0.009	15
1.897	2.107	143.0	0.176	0.009	16
1.929	2.121	143.2	0.164	0.008	16
1.963	2.136	143.4	0.137	0.008	16
1.998	2.152	143.6	0.126	0.008	16
2.034	2.167	143.9	0.101	0.007	16
2.072	2.184	144.1	0.104	0.007	16

Pion-Lab.-Angle: 95 Degree

k_{lab} [GeV]	W_{CM} [GeV]	Θ_{CM} [deg.]	$d\sigma/d\Omega$ [$\mu b/st$]	Error [$\mu b/st$]	#
0.313	1.211	112.3	22.888	0.641	1
0.319	1.216	112.5	20.760	0.603	1
0.324	1.220	112.6	20.839	0.603	1
0.330	1.225	112.8	18.718	0.594	1
0.337	1.230	112.9	18.536	0.534	1
0.343	1.235	113.0	17.155	0.456	2
0.344	1.235	113.1	16.675	0.519	1
0.347	1.238	113.1	16.683	0.417	2
0.352	1.241	113.3	15.877	0.409	2
0.357	1.245	113.4	15.097	0.402	2
0.363	1.250	113.5	13.276	0.399	2
0.369	1.254	113.7	12.709	0.365	2
0.375	1.259	113.8	11.670	0.329	2
0.375	1.259	113.8	11.567	0.291	3
0.381	1.263	113.9	10.474	0.273	3
0.381	1.263	114.0	11.130	0.330	2
0.387	1.268	114.1	10.020	0.274	3
0.393	1.272	114.2	9.440	0.241	3
0.399	1.276	114.4	8.482	0.239	3
0.406	1.282	114.6	7.768	0.221	3
0.413	1.287	114.7	7.443	0.215	4
0.413	1.287	114.7	7.238	0.215	3
0.417	1.290	114.8	6.941	0.216	4
0.421	1.292	114.9	7.144	0.205	3
0.422	1.293	114.9	6.830	0.202	4
0.426	1.296	115.0	6.786	0.203	4
0.431	1.300	115.2	6.135	0.196	4
0.436	1.303	115.3	6.238	0.199	4
0.441	1.307	115.4	6.083	0.187	4
0.446	1.310	115.5	5.714	0.190	4
0.452	1.315	115.7	6.009	0.184	4
0.457	1.318	115.8	5.369	0.190	4
0.461	1.321	115.9	5.336	0.152	5
0.464	1.323	116.0	5.334	0.186	4
0.466	1.325	116.0	5.267	0.149	5
0.470	1.328	116.1	5.149	0.171	4
0.471	1.328	116.1	5.176	0.150	5
0.477	1.332	116.3	4.770	0.143	5
0.483	1.337	116.4	4.849	0.142	5
0.488	1.340	116.6	4.879	0.141	5
0.495	1.345	116.7	4.603	0.137	5
0.501	1.349	116.8	4.451	0.136	5
0.508	1.354	117.0	4.542	0.132	5
0.515	1.359	117.1	4.330	0.131	5
0.516	1.360	117.2	4.432	0.141	6
0.522	1.364	117.3	4.327	0.135	6
0.522	1.364	117.3	4.439	0.130	5
0.528	1.368	117.5	4.436	0.132	6
0.530	1.369	117.5	4.135	0.123	5
0.535	1.373	117.6	4.602	0.133	6

Pion-Lab.-Angle: 95 Degree

k_{lab} [GeV]	W_{CM} [GeV]	Θ_{CM} [deg.]	$d\sigma/d\Omega$ [$\mu b/st$]	Error [$\mu b/st$]	#
0.542	1.377	117.8	4.456	0.126	6
0.549	1.382	117.9	4.291	0.127	6
0.557	1.388	118.1	4.542	0.129	6
0.564	1.392	118.3	4.157	0.124	6
0.573	1.398	118.5	4.265	0.124	6
0.581	1.404	118.6	4.078	0.126	6
0.584	1.406	118.7	4.264	0.129	7
0.590	1.410	118.9	4.257	0.120	6
0.591	1.410	118.9	4.220	0.126	7
0.599	1.416	119.0	4.078	0.126	7
0.600	1.416	119.1	4.163	0.122	6
0.607	1.421	119.2	3.921	0.126	7
0.616	1.427	119.4	4.437	0.128	7
0.625	1.433	119.6	4.162	0.123	7
0.634	1.439	119.8	4.351	0.126	7
0.644	1.445	120.0	4.231	0.121	7
0.654	1.452	120.2	4.700	0.131	7
0.655	1.452	120.2	4.670	0.143	8
0.659	1.455	120.3	4.789	0.140	8
0.664	1.458	120.4	4.924	0.139	8
0.664	1.458	120.4	4.588	0.123	7
0.668	1.461	120.5	4.740	0.137	8
0.673	1.464	120.6	4.843	0.141	8
0.675	1.465	120.6	4.711	0.130	7
0.678	1.467	120.7	4.926	0.140	8
0.683	1.470	120.8	5.044	0.141	8
0.687	1.473	120.9	5.155	0.135	7
0.688	1.474	120.9	5.393	0.142	8
0.694	1.477	121.0	5.476	0.148	8
0.698	1.480	121.1	5.585	0.143	9
0.699	1.481	121.1	5.143	0.144	8
0.703	1.483	121.2	5.689	0.140	9
0.704	1.484	121.2	5.884	0.148	8
0.707	1.486	121.3	5.780	0.139	9
0.709	1.487	121.3	5.738	0.150	8
0.712	1.489	121.4	5.898	0.139	9
0.716	1.491	121.5	5.864	0.150	8
0.718	1.493	121.5	5.700	0.140	9
0.721	1.494	121.6	5.993	0.149	8
0.723	1.496	121.6	5.405	0.133	9
0.727	1.498	121.7	5.686	0.150	8
0.729	1.499	121.7	5.691	0.136	9
0.733	1.502	121.8	5.568	0.143	8
0.735	1.503	121.8	5.447	0.136	9
0.739	1.506	121.9	5.484	0.140	8
0.740	1.506	121.9	5.464	0.133	9
0.746	1.510	122.1	5.661	0.145	8
0.746	1.510	122.0	5.567	0.133	9
0.752	1.514	122.1	5.248	0.138	8
0.752	1.514	122.2	5.142	0.129	9

Pion-Lab.-Angle: 95 Degree

k_{lab} [GeV]	W_{CM} [GeV]	Θ_{CM} [deg.]	$d\sigma/d\Omega$ [$\mu b/st$]	Error [$\mu b/st$]	#
0.758	1.517	122.3	5.141	0.128	9
0.758	1.517	122.3	4.987	0.139	8
0.765	1.522	122.4	4.858	0.124	9
0.766	1.522	122.4	4.828	0.132	8
0.771	1.526	122.5	4.737	0.123	9
0.772	1.526	122.5	4.538	0.127	8
0.778	1.530	122.6	4.559	0.119	9
0.780	1.531	122.7	4.329	0.125	8
0.784	1.533	122.8	4.211	0.114	9
0.787	1.535	122.8	4.138	0.125	8
0.791	1.538	122.9	4.046	0.116	9
0.798	1.542	123.0	4.045	0.112	9
0.805	1.546	123.1	3.822	0.108	9
0.811	1.550	123.2	3.831	0.104	10
0.812	1.551	123.2	3.537	0.108	9
0.817	1.554	123.3	3.685	0.101	10
0.821	1.556	123.4	3.489	0.102	9
0.824	1.558	123.5	3.530	0.102	10
0.828	1.560	123.5	3.296	0.101	9
0.830	1.561	123.6	3.493	0.098	10
0.836	1.565	123.6	2.931	0.098	9
0.837	1.566	123.7	3.249	0.095	10
0.844	1.570	123.8	3.194	0.098	10
0.844	1.570	123.8	3.025	0.093	9
0.851	1.574	123.9	3.071	0.094	10
0.859	1.579	124.1	3.123	0.089	10
0.866	1.583	124.2	3.078	0.088	10
0.873	1.587	124.3	3.201	0.093	10
0.881	1.592	124.4	3.063	0.091	10
0.889	1.596	124.6	3.061	0.089	10
0.897	1.601	124.7	3.088	0.088	10
0.905	1.606	124.8	3.057	0.091	10
0.914	1.611	125.0	3.159	0.089	10
0.923	1.616	125.1	2.961	0.089	10
0.932	1.622	125.3	3.133	0.089	10
0.941	1.627	125.4	3.358	0.090	10
0.950	1.632	125.5	3.304	0.087	10
0.959	1.637	125.7	3.361	0.092	10
0.969	1.643	125.8	3.549	0.063	11
0.969	1.643	125.8	3.389	0.093	10
0.978	1.648	126.0	3.467	0.062	11
0.979	1.648	126.0	3.578	0.093	10
0.986	1.652	126.1	3.576	0.062	11
0.990	1.655	126.2	3.415	0.093	10
0.996	1.658	126.3	3.565	0.063	11
1.005	1.663	126.4	3.579	0.062	11
1.015	1.669	126.6	3.499	0.062	11
1.025	1.674	126.7	3.393	0.060	11
1.035	1.680	126.8	3.226	0.059	11
1.044	1.685	127.0	2.874	0.055	11

Pion-Lab.-Angle: 95 Degree

k_{lab} [GeV]	W_{CM} [GeV]	Θ_{CM} [deg.]	$d\sigma/d\Omega$ [$\mu b/st$]	Error [$\mu b/st$]	#
1.056	1.692	127.2	2.669	0.054	11
1.067	1.698	127.3	2.509	0.051	11
1.077	1.703	127.4	2.204	0.049	11
1.090	1.711	127.7	1.887	0.045	11
1.101	1.717	127.8	1.700	0.043	11
1.113	1.723	128.0	1.481	0.040	11
1.126	1.730	128.2	1.257	0.037	11
1.138	1.737	128.3	1.067	0.035	11
1.138	1.737	128.3	1.149	0.036	12
1.149	1.743	128.4	0.953	0.034	12
1.151	1.744	128.5	0.927	0.034	11
1.162	1.750	128.6	0.931	0.032	12
1.173	1.755	128.8	0.855	0.030	12
1.186	1.762	129.0	0.721	0.030	12
1.199	1.769	129.1	0.693	0.028	12
1.212	1.776	129.3	0.659	0.028	12
1.226	1.784	129.5	0.713	0.028	12
1.240	1.791	129.6	0.652	0.027	12
1.255	1.799	129.9	0.583	0.026	12
1.269	1.806	130.0	0.628	0.026	12
1.285	1.814	130.2	0.647	0.026	12
1.301	1.823	130.4	0.683	0.024	12
1.317	1.831	130.6	0.682	0.025	12
1.318	1.831	130.6	0.689	0.024	13
1.332	1.838	130.7	0.709	0.025	13
1.333	1.839	130.8	0.684	0.024	12
1.349	1.847	131.0	0.711	0.024	13
1.364	1.855	131.1	0.694	0.024	13
1.381	1.863	131.3	0.705	0.024	13
1.399	1.872	131.5	0.686	0.023	13
1.415	1.880	131.7	0.702	0.023	13
1.435	1.890	132.0	0.668	0.023	13
1.452	1.899	132.1	0.656	0.022	13
1.472	1.909	132.3	0.661	0.023	13
1.494	1.919	132.6	0.609	0.021	13
1.506	1.925	132.7	0.649	0.018	14
1.513	1.929	132.8	0.614	0.020	13
1.521	1.933	132.8	0.592	0.017	14
1.541	1.942	133.0	0.575	0.017	14
1.561	1.952	133.2	0.538	0.016	14
1.582	1.962	133.5	0.509	0.015	14
1.606	1.973	133.7	0.500	0.015	14
1.627	1.983	133.9	0.436	0.015	14
1.652	1.995	134.1	0.418	0.014	14
1.675	2.006	134.4	0.364	0.014	14
1.682	2.009	134.4	0.386	0.009	15
1.700	2.018	134.6	0.347	0.013	14
1.704	2.019	134.6	0.345	0.008	15
1.727	2.030	134.8	0.319	0.008	15
1.754	2.043	135.1	0.270	0.008	15

Pion-Lab.-Angle: 95 Degree

k_{lab} [GeV]	W_{CM} [GeV]	Θ_{CM} [deg.]	$d\sigma/d\Omega$ [$\mu b/st$]	Error [$\mu b/st$]	#
1.782	2.055	135.4	0.230	0.007	15
1.807	2.067	135.5	0.206	0.007	15
1.836	2.080	135.8	0.201	0.007	15
1.838	2.081	135.8	0.190	0.007	16
1.864	2.092	136.0	0.176	0.006	15
1.865	2.093	136.0	0.171	0.007	16
1.891	2.105	136.2	0.153	0.007	16
1.922	2.118	136.5	0.127	0.006	16
1.953	2.132	136.8	0.115	0.006	16
1.986	2.146	137.0	0.109	0.006	16
2.018	2.160	137.3	0.100	0.005	16
2.047	2.173	137.5	0.098	0.005	16

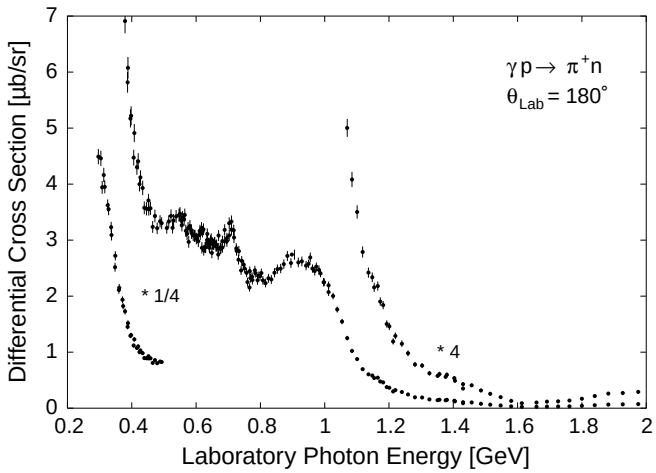

Fig. 9. Differential cross-section for $\gamma p \to \pi^+ n$ at a laboratory pion angle of $\Theta = 180°$ as a function of the laboratory photon energy. The data around the first resonance are reduced to 1/4 and above the third resonance the cross-sections are in addition plotted after multiplication by 4.

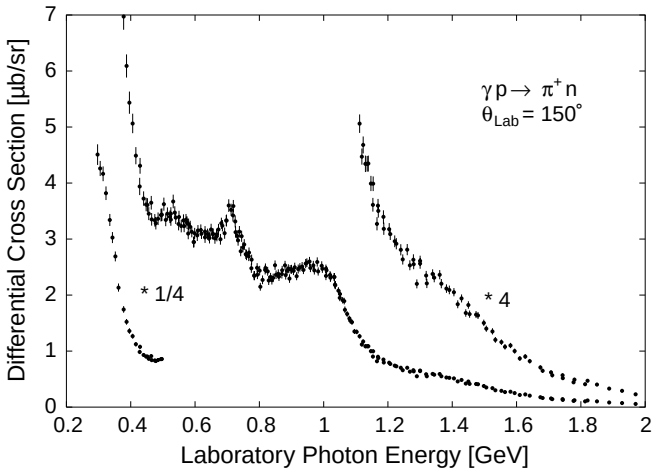

Fig. 10. Differential cross-section for $\gamma p \to \pi^+ n$ at a laboratory pion angle of $\Theta = 150°$ as a function of the laboratory photon energy. The data around the first resonance are reduced to 1/4 and above the third resonance the cross-sections are in addition plotted after multiplication by 4.

increases again. Centered at the threshold for the η-photoproduction $\gamma p \to \eta p$ at 0.71 GeV there appears a sharp spike. The following dip is complementary to the η-photoproduction cross-section which has its maximum around 0.8 GeV and then drops rapidly to 20% of the maximum value above 0.9 GeV. In a simple picture, the observed phenomenon can be explained by a strong excitation of the $S_{11}(1535)$ resonance which above the η-production threshold at 0.71 GeV predominantly decays into $p+\eta$, and thus, by unitarity, causes a discontinuity in the pion-nucleon channel. This η-cusp in $\gamma p \to \pi^+ n$ was reported earlier by Hand and Schaerf [13]. A more detailed investigation of this effect was given in ref. [14].

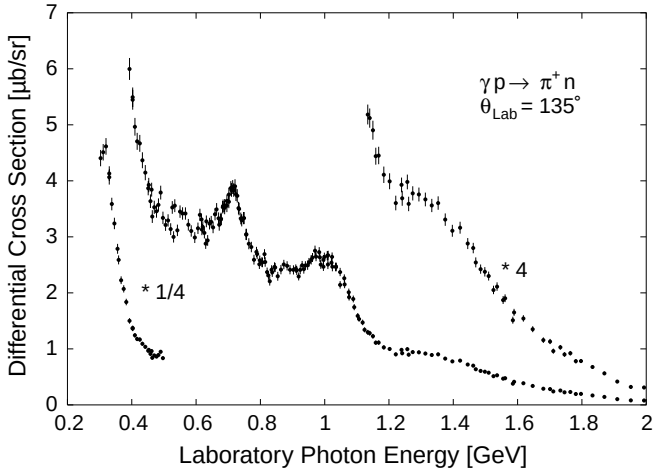

Fig. 11. Differential cross-section for $\gamma p \to \pi^+ n$ at a laboratory pion angle of $\Theta = 135°$ as a function of the laboratory photon energy. The data around the first resonance are reduced to 1/4 and above the third resonance the cross-sections are in addition plotted after multiplication by 4.

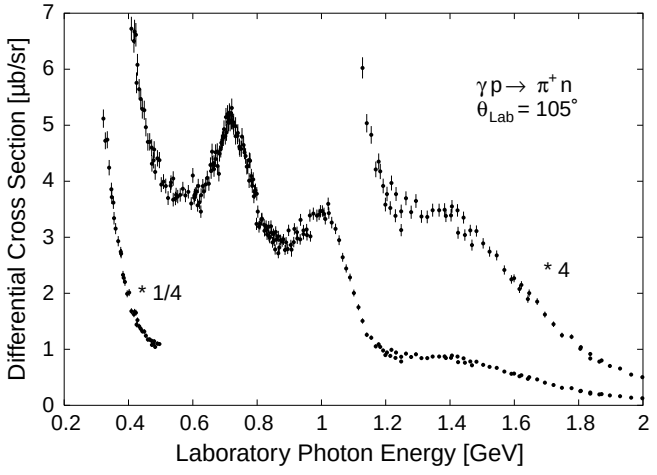

Fig. 13. Differential cross-section for $\gamma p \to \pi^+ n$ at a laboratory pion angle of $\Theta = 105°$ as a function of the laboratory photon energy. The data around the first resonance are reduced to 1/4 and above the third resonance the cross-sections are in addition plotted after multiplication by 4.

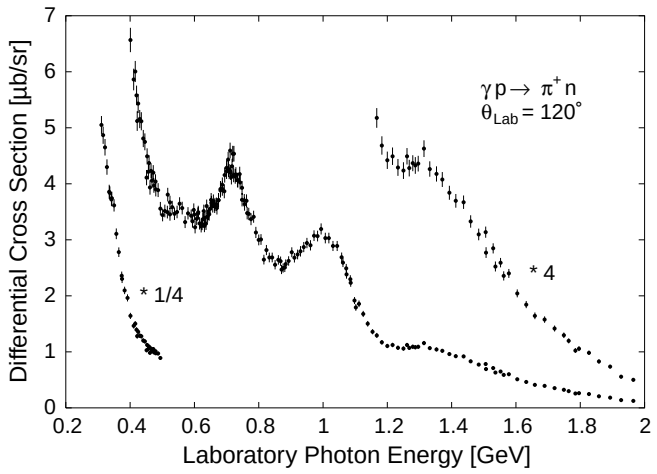

Fig. 12. Differential cross-section for $\gamma p \to \pi^+ n$ at a laboratory pion angle of $\Theta = 120°$ as a function of the laboratory photon energy. The data around the first resonance are reduced to 1/4 and above the third resonance the cross-sections are in addition plotted after multiplication by 4.

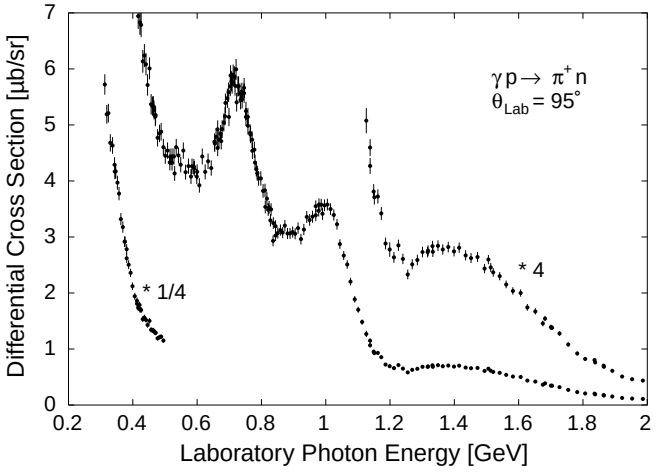

Fig. 14. Differential cross-section for $\gamma p \to \pi^+ n$ at a laboratory pion angle of $\Theta = 95°$ as a function of the laboratory photon energy. The data around the first resonance are reduced to 1/4 and above the third resonance the cross-sections are in addition plotted after multiplication by 4.

Changing to a laboratory angle of 150° (fig. 10) we find a similar behaviour of the measured cross-section up to about 1.1 GeV, except for the η-cusp region where the observed structure is shifted to higher cross-section values because of the build-up of the second resonance. The most striking feature is the steep increase with decreasing angle at energies around 1.25 GeV. At the laboratory angles of 135°, 120°, 105° and 95° (figs. 11 to 14) we find a slow increase of the cross-section at the first resonance. The second resonance is growing much stronger towards smaller angles. At all angles the opening of the η-channel shows up as an almost linear decrease of the cross-section above 0.71 GeV on top of the second resonance. We notice a moderate growth of the cross-section at the position of the third resonance at 1.0 GeV. At photon energies of 1.35 GeV the cross-section increases strongly towards smaller angles, reaches a maximum at a laboratory angle of 120°, and then drops again towards 95°.

5.2 Comparison with existing data and the recent SAID analysis

At photon energies below 2 GeV a large number of experiments has been carried out over the last four decades. In the following, we will restrict our discussion to the measurements which were accepted to the data base for the SAID analysis carried out by Arndt, Strakovsky and Workman [15]. Our results in the region of the first resonance at six different laboratory angles are plotted in

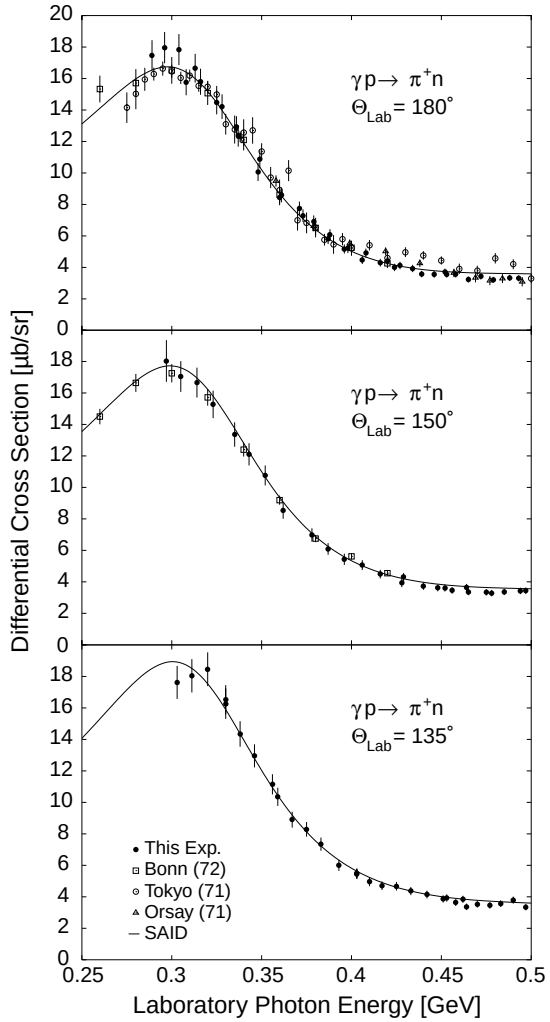

Fig. 15. The results of this experiment in the region of the first resonance in comparison with the SAID analysis and data from Bonn [16], Tokyo [18] and Orsay [17].

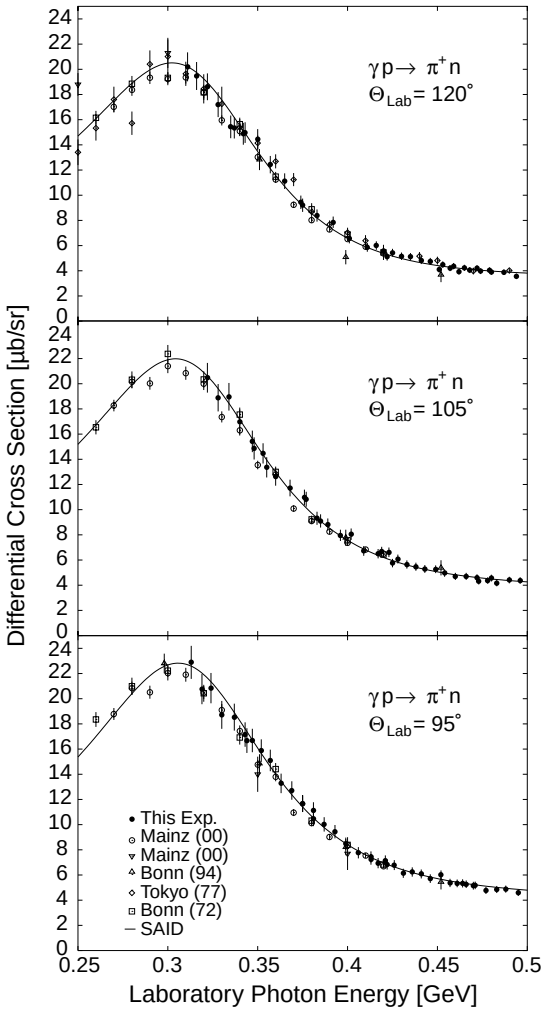

Fig. 16. The results of this experiment in the region of the first resonance in comparison with the SAID analysis and data from Mainz [20], Mainz [21], Bonn [16], Tokyo [19] and Bonn [22].

figs. 15 and 16 together with the curves of the recent SAID analysis. (The error bars given here also include the systematic uncertainties.) In addition, the results of measurements from Tokyo, Orsay, Mainz and Bonn are shown. Within the experimental uncertainties our data agree quite well with the SAID results. This is also true for the earlier Bonn results [16]. At the laboratory angle of 180° there are data from two dedicated experiments carried out at Orsay [17] and Tokyo [18]. Around the maximum of the first resonance the Tokyo values in general agree with the SAID curves. Above 400 MeV, however, we notice larger deviations. With a few exceptions, the Orsay data are in agreement with the SAID analysis.

At smaller laboratory angles there are further contributions from Tokyo, Mainz and Bonn. The Tokyo results [19] for $\Theta_{\rm Lab} = 120°$ follow within the quoted uncertainties the SAID curve with a few exceptions. At $\Theta_{\rm Lab} = 120°$ and the two smaller laboratory angles there are data from two Mainz experiments [20,21]. Along the high-energy tails of the first resonance these values follow closely the SAID curves. Around the resonance maximum there seems to be a slight difference in normalisation. The Bonn data [22] at 400 MeV and 450 MeV agree very well for $\Theta_{\rm Lab} = 105°$ and $\Theta_{\rm Lab} = 95°$, whereas at $\Theta_{\rm Lab} = 120°$ there are sizeable deviations. A comparison of our data at photon energies between 450 and 1250 MeV with the SAID analysis is given in figs. 17 to 22. The error bars shown here also include the systematic uncertainties. The data from Orsay, Tokyo, Cornell and MIT are also plotted.

In general, our data follow the course of the SAID excitation curves very well, though there are also a few local deviations. The measurements at the laboratory angle of 180° are shown in fig. 17. At the low-energy side, the Tokyo data [18] show considerable deviations, but good agreement above 700 MeV. The Orsay [17] results indicate a similar behaviour. At photon energies above 660 MeV there are data from a further dedicated 180° measurement carried out at Cornell [23]. In the beginning they agree with the SAID results, but above 800 MeV are large deviations. At the smaller laboratory angles of $\Theta_{\rm Lab} = 135°$ and $\Theta_{\rm Lab} = 95°$ the Tokyo data [19] are

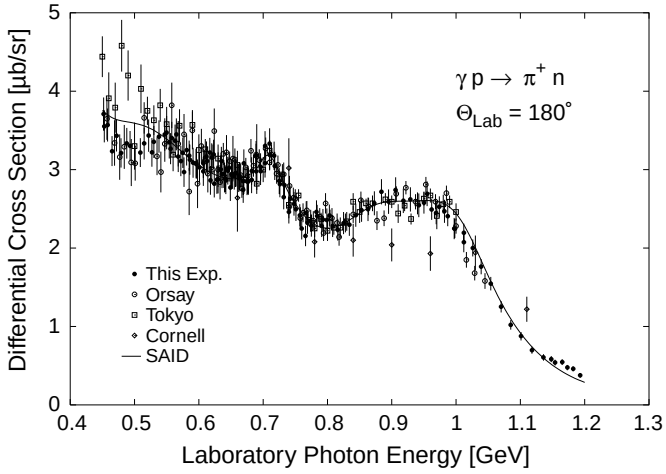

Fig. 17. The results of this experiment in the medium energy range at the laboratory angle of 180° compared with the SAID analysis and data from Orsay [17], Tokyo [18] and Cornell [23].

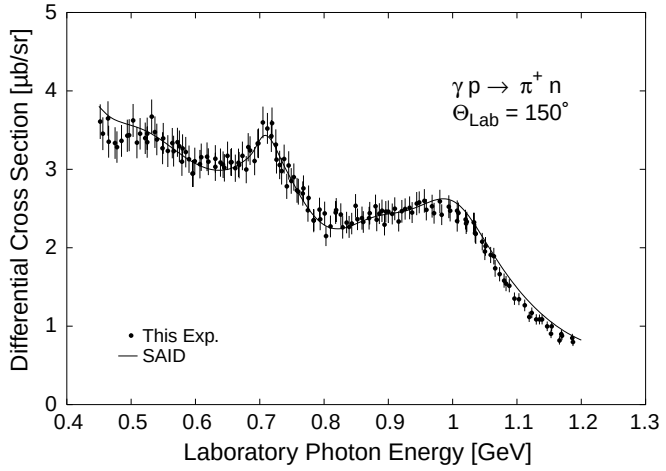

Fig. 18. The results of this experiment in the medium energy range at the laboratory angle of 150° compared with the SAID analysis.

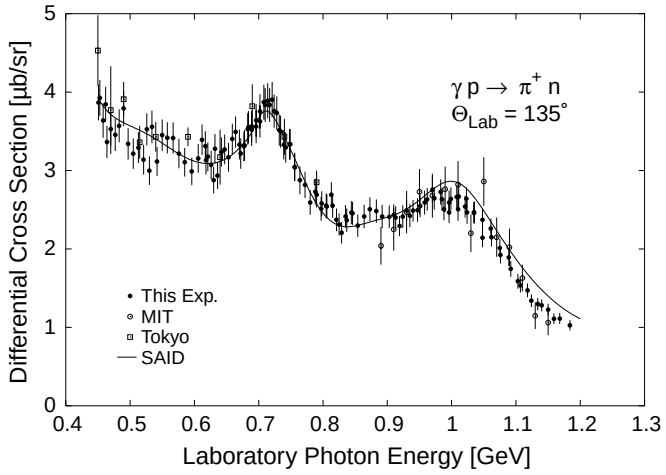

Fig. 19. The results of this experiment in the medium energy range at the laboratory angle of 135° compared with the SAID analysis and data from MIT [25] and Tokyo [19].

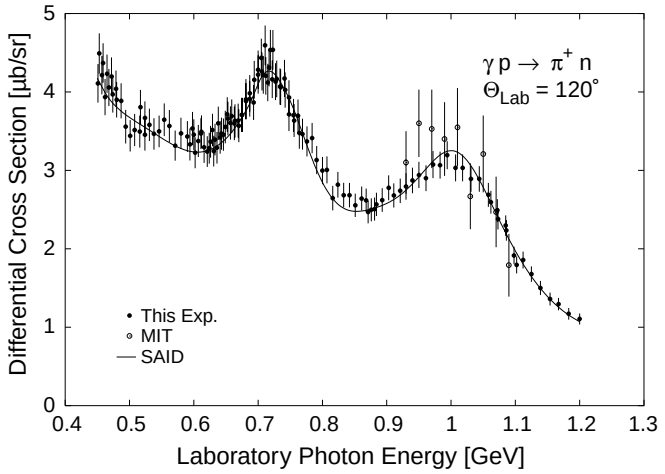

Fig. 20. The results of this experiment in the medium energy range at a laboratory angle of 120° compared with the SAID analysis and data from MIT [19].

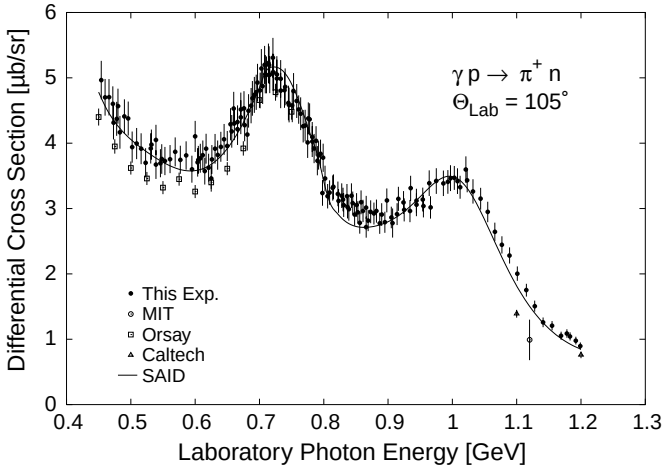

Fig. 21. The results of this experiment in the medium energy range at a laboratory angle of 105° compared with the SAID analysis and data from Orsay [24].

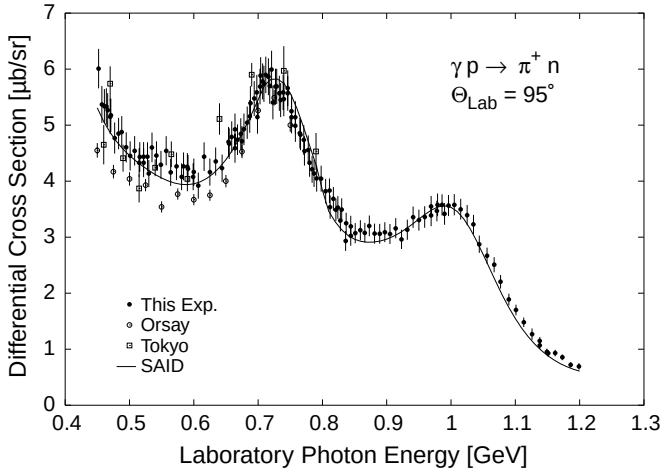

Fig. 22. The results of this experiment in the medium energy range at a laboratory angle of 95° compared with the SAID analysis and data from Orsay [24] and Tokyo [19].

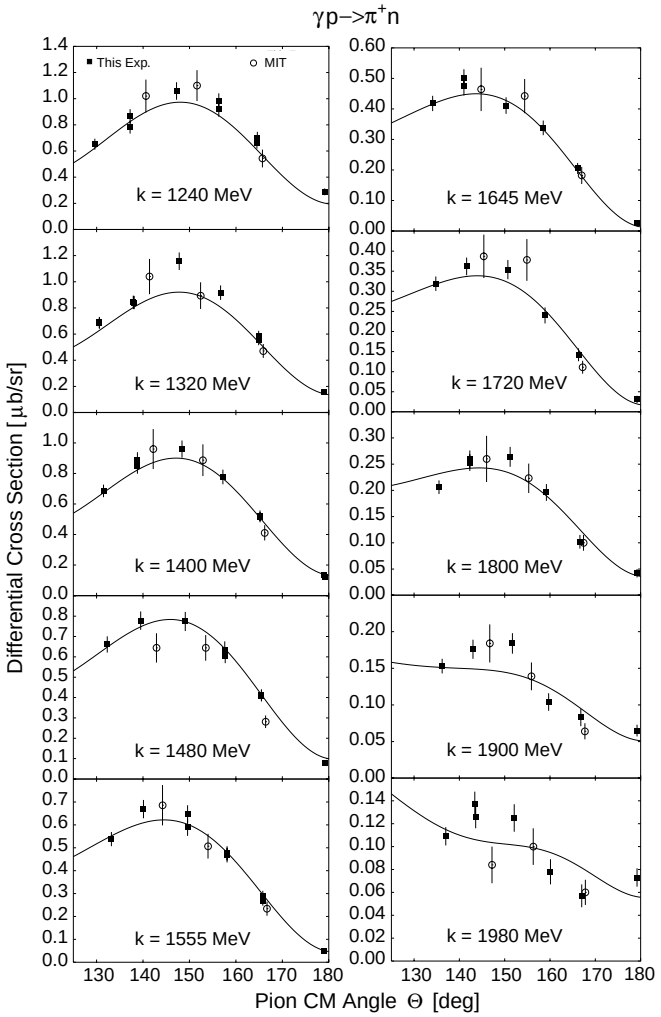

Fig. 23. CM angular distributions at backward angles for photon energies between 1.240 MeV (GeV) and 1.980 MeV (GeV). The results of this experiment are plotted together with the data from MIT [25]. The curves show the results of the SAID analysis.

systematically above the SAID curves, whereas the Orsay values [24] at $\Theta_{\rm Lab} = 105°$ and $\Theta_{\rm Lab} = 95°$ are always below the analysis. The values of MIT [25] at $\Theta_{\rm Lab} = 135°$ and $\Theta_{\rm Lab} = 120°$ are in agreement with the SAID curves, but they show partly large uncertainties. The MIT group measured three excitation curves at three fixed laboratory angles in the backward hemisphere above photon energies of 0.900 GeV. Part of their data between 1.2 GeV and 1.98 GeV are plotted as angular distributions at ten fixed photon energies in fig. 23 together with our cross-sections at the corresponding energies. Again the curves give the results of the SAID analysis. Within the experimental uncertainties the two data sets agree with the analysis, except at the two highest energies where the combined data sets indicate a different shape of the angular distributions.

We are indebted to the synchrotron group and the computer staff for their excellent support during the experiment. Our thanks go further to the technicians and members of the machine shop for their great help in the setting-up and maintenance of the experimental equipment. Useful discussions with Walter Pfeil are gratefully acknowledged. The authors are grateful to Frank Frommberger for providing many diagrams and Beate von Roy for valuable help in preparing this publication. Finally, we would like to thank our colleagues P.J. Kasper, K. Kircher and U. Schaefer for their help during the experiment. Financial support was provided by the Bundesministerium für Bildung, Wissenschaft, Forschung und Technologie.

References

1. D. Menze, W. Pfeil, R. Wilcke, Compilation of Pion Photoproduction Data, ZAED-PHYSICS DATA 7-1 (1977); K. Ukai, T. Nakamura, Data Compilation of Single Pion Photoproduction Below 2 GeV, University of Tokyo, INS-T-550 (1997).
2. Particle Data Group, *Review of Particle Physics*, Eur. Phys. J. C **15**, 698 (2000).
3. M. Leneke, Ph.D. thesis, Bonn University 1977, BONN-IR-77-14; H.-W. Dannhausen, Ph.D. thesis, Bonn University 1977, BONN-IR-77-29.
4. K.H. Althoff et al., Nucl. Instrum. Methods **61**, 1 (1968).
5. R.R. Wilson, Nucl. Instrum. Methods **1**, 100 (1957); H. Stein, R. Wedemeyer, Internal Report, Bonn UNIV-PIB 1-109 (1970).
6. D. Lublow, DESY-Notiz A 2.96 (1963).
7. G. Lutz, H.D. Schultz, DESY Report 67/29 (1967).
8. V. Eckardt, DESY Report 67/12 (1967); B. Niemann, BONN UNIV. IR-76-28 (1976).
9. J. Dupin, Ph.D. thesis, Université de Paris, Jan. 1967.
10. H.A. Thiessen, Phys. Rev. **155**, 1488 (1967).
11. B. d'Almagne, Ph.D. thesis, Université de Paris, Orsay Report, L.A.L. 1239 (1970).
12. R.L. Walker, Phys. Rev. **182**, 1729 (1967).
13. L. Hand, C. Schaerf, Phys. Rev. Lett. **6**, 229 (1961).
14. K.H. Althoff et al., Z. Phys. C **1**, 327 (1979).
15. R.A. Arndt, I.I. Strakovsky, R.L. Workman, Phys. Rev. C **53**, 430 (1996).
16. G. Fischer et al., Z. Phys. **253**, 38 (1972).
17. B. Bouquet et al., Phys. Rev. Lett. **27**, 1244 (1972).
18. T. Fujii et al., Phys. Rev. Lett. **26**, 1672 (1971).
19. T. Fujii et al., Nucl. Phys. B **120**, 395 (1977).
20. R. Beck et al., Phys. Rev. C **61**, 035204 (2000).
21. D. Branford et al., Phys. Rev. C **61**, 014603 (2000).
22. K. Büchler et al., Nucl. Phys. A **570**, 580 (1994).
23. K. Ekstrand, A. Browman, L. Hand, M.E. Nordberg, Phys. Rev. D **6**, 1 (1972).
24. C. Betourne et al., Phys. Rev. **172**, 1343 (1968).
25. R.A. Alvarez et al., Phys. Rev. D **1**, 1946 (1970).